

An Enhanced SDR based Global Algorithm for Nonconvex Complex Quadratic Programs with Signal Processing Applications

Cheng Lu, Ya-Feng Liu, and Jing Zhou

Abstract—In this paper, we consider a class of nonconvex complex quadratic programming (CQP) problems, which find a broad spectrum of signal processing applications. By using the polar coordinate representations of the complex variables, we first derive a new enhanced semidefinite relaxation (SDR) for problem (CQP). Based on the newly derived SDR, we further propose an efficient branch-and-bound algorithm for solving problem (CQP). Key features of our proposed algorithm are: (1) it is guaranteed to find the global solution of the problem (within any given error tolerance); (2) it is computationally efficient because it carefully utilizes the special structure of the problem. We apply our proposed algorithm to solve the multi-input multi-output (MIMO) detection problem, the unimodular radar code design problem, and the virtual beamforming design problem. Simulation results show that our proposed enhanced SDR, when applied to the above problems, is generally much tighter than the conventional SDR and our proposed global algorithm can efficiently solve these problems. In particular, our proposed algorithm significantly outperforms the state-of-the-art sphere decode algorithm for solving the MIMO detection problem in the hard cases (where the number of inputs and outputs is equal or the signal-to-noise-ratio is low) and a state-of-the-art general-purpose global optimization solver called Baron for solving the virtual beamforming design problem.

Index Terms—Branch-and-bound algorithm, enhanced SDR, MIMO detection, nonconvex CQP, virtual beamforming.

I. INTRODUCTION

In this paper, we consider the following nonconvex complex quadratic programming problem:

$$\begin{aligned} \min_{\mathbf{x} \in \mathbb{C}^n} \quad & F(\mathbf{x}) := \frac{1}{2} \mathbf{x}^\dagger \mathbf{Q} \mathbf{x} + \text{Re}(\mathbf{c}^\dagger \mathbf{x}) \\ \text{s.t.} \quad & \ell_i \leq |x_i| \leq u_i, \quad i = 1, 2, \dots, n, \\ & \arg(x_i) \in \mathcal{A}_i, \quad i = 1, 2, \dots, n, \end{aligned} \quad (\text{CQP})$$

The work of C. Lu was supported by the National Natural Science Foundation of China (NSFC) under Grant 11701177 and Grant 11771243. The work of Y.-F. Liu was supported in part by the NSFC under Grant 11991021, Grant 11688101, Grant 11671419, and Grant 11631013. The work of J. Zhou was supported by the NSFC under Grant 11701512. Part of this work [1] has been presented (as an invited paper) at the IEEE International Conference on Communications in China (ICCC), Qingdao, China, October 22–24, 2017. (Corresponding author: Ya-Feng Liu.)

C. Lu is with the School of Economics and Management, North China Electric Power University, Beijing 102206, China (e-mail: lucheng1983@163.com). Y.-F. Liu is with the State Key Laboratory of Scientific and Engineering Computing, Institute of Computational Mathematics and Scientific/Engineering Computing, Academy of Mathematics and Systems Science, Chinese Academy of Sciences, Beijing 100190, China (e-mail: yafliu@lsec.cc.ac.cn). J. Zhou is with the Department of Applied Mathematics, College of Science, Zhejiang University of Technology, Hangzhou 310023, China (e-mail: zhoujing@zjut.edu.cn).

where

- $\mathbf{x} = [x_1, x_2, \dots, x_n]^\top \in \mathbb{C}^n$ is the n -dimensional complex (unknown) variable;
- $\mathbf{Q} \in \mathbb{C}^{n \times n}$ is a Hermitian matrix, $\mathbf{c} \in \mathbb{C}^n$ is a complex vector, u_i and ℓ_i ($i = 1, 2, \dots, n$), satisfying $u_i \geq \ell_i \geq 0$, are $2n$ real numbers, and \mathcal{A}_i ($i = 1, 2, \dots, n$) are n discrete/continuous sets; and
- $\text{Re}(\cdot)$, $|\cdot|$, and $\arg(\cdot)$ denote the real part, the magnitude, and the argument of a complex number, and $(\cdot)^\top$ and $(\cdot)^\dagger$ denote the transpose and Hermitian transpose of a (complex) vector.

Problem (CQP) finds many important signal processing applications, including multi-input multi-output (MIMO) detection [2], [3], unimodular radar code design [4], [5], [6], virtual beamforming [7], phase recovery [8], sensor bias estimation [9], and angular synchronization [10]; see Section II further ahead. For more applications of problem (CQP) in signal processing and communications, please refer to [11] and [12] and references therein. In addition, problem (CQP) has also attracted much attention in the mathematical programming community [13], [14], [15], [16], [17], [18]. For instance, some well-known combinatorial optimization problems, including the max-cut problem [16] and the max-3-cut problem [17], and the so-called unit-modulus constrained QP [15] can all be recast into the form of problem (CQP).

It is known that problem (CQP) is NP-hard in general [14]. Hence, there is no polynomial time algorithm which can solve it to global optimality (unless P=NP). Most of existing algorithms for solving problem (CQP) are approximation algorithms, local optimization algorithms, or other heuristics (e.g., [3], [4], [5], [8], [10], [11], [13], [14], [19], [20], [21]). These algorithms generally cannot guarantee to find the global solutions of problem (CQP), except only for some special cases [9], [10], [22], [23]. A straightforward way of globally solving problem (CQP) is to first reformulate the problem as an equivalent real QP by representing the complex variables by their real and imaginary components and then apply the existing general-purpose global algorithms (e.g., algorithms proposed in [24], [25]) for solving the equivalent real reformulation. However, an issue of doing so is the computational efficiency (see our numerical results in Section V-E), since it does not utilize the special structure of the problem with the complex variables.

To the best of our knowledge, there is no global algorithm that is specially designed and can efficiently solve problem

(CQP) by utilizing the special structure of the problem. The goal of this paper is to fill this gap, i.e., propose an efficient¹ global algorithm for solving problem (CQP). The main contributions of this paper are twofold.

- *A New and Enhanced SDR for Problem (CQP)*. We first give an equivalent reformulation of problem (CQP) by using the polar coordinate representations of the complex variables. The equivalent reformulation reveals the intrinsic nonconvexity of problem (CQP). Then, we derive the *convex envelope*² of these nonconvex constraints in the reformulation and use their convex envelopes to replace the original nonconvex constraints, which thus lead to a new SDR for problem (CQP). The new SDR for problem (CQP) is generally (much) tighter than the conventional SDR, which directly drops the nonconvex constraints in the equivalent reformulation. It is worth mentioning that the new enhanced SDR for problem (CQP) is computationally very efficient as all newly added constraints as compared with the conventional SDR are linear constraints.
- *An Efficient Global Algorithm for Problem (CQP)*. Based on the newly derived SDR, we propose an efficient branch-and-bound algorithm for problem (CQP) that is guaranteed to find its global solution (within any given error tolerance). The newly derived SDR plays a very crucial role in the proposed branch-and-bound algorithm, because the algorithm needs to solve an SDR at each iteration and the optimal values of all solved SDRs will provide a lower bound for problem (CQP). We emphasize here that the efficiency of a branch-and-bound algorithm considerably relies on the quality of the lower bound. To the best of our knowledge, our proposed branch-and-bound algorithm is the first tailored algorithm for globally solving problem (CQP).

We apply our proposed branch-and-bound algorithm to solve three important signal processing problems, i.e., the MIMO detection problem [2], [3], the unimodular radar code design problem [4], [5], [6], and the virtual beamforming design problem [7]. Simulation results show that our proposed new SDR, when applied to these problems, is indeed generally much tighter than the conventional SDR. Moreover, simulation results show that our proposed global algorithm is highly efficient and outperforms the state-of-the-art algorithm/solver for solving these problems. More specifically, our proposed algorithm can solve the MIMO detection problem in case of 8-PSK and with the number of inputs and outputs n and m being 20 and signal-to-noise-ratio (SNR) being 5 dB within 140 seconds (on average) while the state-of-the-art sphere decode algorithm [26], [27] needs 1836 seconds; our proposed algorithm can solve the virtual beamforming design problem with $m = 10$ and $n = 5$ within 0.09 seconds while the state-of-the-art general-purpose global optimization solver Baron [25] needs more than 80 seconds.

¹The term “efficient” in this paper means that the corresponding algorithm is computationally efficient, which does not imply that the algorithm has a polynomial time complexity.

²For a given set, its convex envelope is defined as the smallest convex set that contains it.

We adopt the following notations throughout the paper. We use lowercase boldface and uppercase boldface letters to denote (column) vectors and matrices, respectively. For a given complex vector $\mathbf{x} \in \mathbb{C}^n$, $\|\mathbf{x}\|_2$ denotes its Euclidean norm and $\text{Re}(\mathbf{x})$ and $\text{Im}(\mathbf{x})$ denote its component-wise real and imaginary part, respectively. For a given complex Hermitian matrix \mathbf{A} , $\mathbf{A} \succeq \mathbf{0}$ means \mathbf{A} is positive semidefinite. For two given Hermitian matrices \mathbf{A} and \mathbf{B} , $\mathbf{A} \succeq \mathbf{B}$ means $\mathbf{A} - \mathbf{B} \succeq \mathbf{0}$. Moreover, let $\text{Trace}(\cdot)$ denote the trace operator, let $\mathbf{A} \bullet \mathbf{B}$ denote $\text{Trace}(\mathbf{A}^\dagger \mathbf{B})$ (i.e., $\sum_i \sum_j A_{ij} B_{ij}$, where A_{ij} denotes the (i, j) -th entry of matrix \mathbf{A}), and let $\|\mathbf{A}\|_F$ denote $\sqrt{\mathbf{A} \bullet \mathbf{A}}$. Finally, we use ν^* to denote the optimal value of problem (CQP).

II. THREE SIGNAL PROCESSING APPLICATIONS OF PROBLEM (CQP)

In this section, we list three important signal processing applications of problem (CQP) and we will focus on these three applications throughout the paper.

■ **MIMO detection** [2], [3]. The input-output relationship of the MIMO channel can be modeled as $\mathbf{r} = \mathbf{H}\mathbf{x} + \mathbf{v}$, where $\mathbf{H} \in \mathbb{C}^{m \times n}$ is the complex channel matrix (for n inputs and m outputs with $m \geq n$), $\mathbf{v} \in \mathbb{C}^m$ is the additive white Gaussian noise, $\mathbf{r} \in \mathbb{C}^m$ is the vector of received signals, and $\mathbf{x} \in \mathbb{C}^n$ is the vector of transmitted symbols. Assume the M -Phase-Shift Keying (PSK) modulation scheme with $M \geq 2$ is adopted. Then, each entry x_i of \mathbf{x} belongs to a finite set of symbols, i.e., $x_i \in \{\exp(i\theta) \mid \theta \in \mathcal{A}\}$, where i is the imaginary unit satisfying $i^2 = -1$ and

$$\mathcal{A} = \{\theta \mid \theta = 2k\pi/M, k = 0, 1, \dots, M-1\}.$$

The maximum likelihood MIMO detection problem is

$$\begin{aligned} \min_{\mathbf{x} \in \mathbb{C}^n} \quad & \frac{1}{2} \|\mathbf{H}\mathbf{x} - \mathbf{r}\|_2^2 \\ \text{s.t.} \quad & |x_i| = 1, \arg(x_i) \in \mathcal{A}, i = 1, 2, \dots, n. \end{aligned} \quad (1)$$

It is clear that problem (1) is a special case of problem (CQP) with $\mathbf{Q} = \mathbf{H}^\dagger \mathbf{H}$, $\mathbf{c} = -\mathbf{H}^\dagger \mathbf{r}$, $\ell_i = u_i = 1$, $\mathcal{A}_i = \mathcal{A}$, $i = 1, 2, \dots, n$. In this case, all of \mathcal{A}_i in problem (CQP) are discrete sets.

■ **Unimodular radar code design** [4], [5], [6]. The goal of the unimodular radar code design problem is to maximize the system's detection performance under the similarity constraint (for controlling the ambiguity distortion). It has been shown (e.g., in [4]) that the system's detection performance depends on the radar code, the disturbance covariance matrix, and the temporal steering vector only through the SNR. Mathematically, the SNR of the considered radar system can be expressed as

$$c \cdot \mathbf{x}^\dagger \left(\mathbf{M}^{-1} \odot (\mathbf{p}\mathbf{p}^\dagger)^* \right) \mathbf{x},$$

where c is a constant (depending only on the cases of the non-fluctuating and fluctuating target), $\mathbf{x} \in \mathbb{C}^n$ is the unimodular radar code to be designed, \mathbf{M} is the positive definite covariance matrix of some unknown zero-mean complex Gaussian noise vector, $\mathbf{p} = [1, e^{i2\pi f_d T_r}, \dots, e^{i2\pi(n-1)f_d T_r}]^\top$ is the temporal steering vector with f_d being the target Doppler frequency, T_r

being the pulse repetition time, and N being the length of the radar code. In the above, \odot denotes the Hadamard product operator, $(\cdot)^{-1}$ denotes the (matrix) inverse operator, and $(\cdot)^*$ denotes the element-wise conjugate operator. The unimodular radar code design problem can be formulated as

$$\begin{aligned} \max_{\mathbf{x} \in \mathbb{C}^n} \quad & \mathbf{x}^\dagger \left(\mathbf{M}^{-1} \odot (\mathbf{p}\mathbf{p}^\dagger)^* \right) \mathbf{x} \\ \text{s.t.} \quad & |x_i| = 1, \quad i = 1, 2, \dots, n, \\ & \|\mathbf{x} - \mathbf{x}^0\|_\infty \leq \delta, \end{aligned} \quad (2)$$

where $\mathbf{x}^0 \in \{\mathbf{x} \in \mathbb{C}^n \mid |x_i| = 1, i = 1, 2, \dots, n\}$ is a predefined desired radar code (e.g., the Barker code) and $\delta > 0$ is a given similarity tolerance. When the tolerance δ is small enough (e.g., $\delta < \sqrt{2}$), the constraint $\|\mathbf{x} - \mathbf{x}^0\|_\infty \leq \delta$ is equivalent to $\arg(x_i) \in [\underline{\theta}_i, \bar{\theta}_i]$ for all $i = 1, 2, \dots, n$, where

$$\begin{aligned} \underline{\theta}_i &= \arg(x_i^0) - \arccos(1 - \delta^2/2), \\ \bar{\theta}_i &= \arg(x_i^0) + \arccos(1 - \delta^2/2). \end{aligned}$$

Therefore, the above unimodular radar code design problem (2) is also a special case of problem (CQP) with $\mathbf{Q} = -2\mathbf{M}^{-1} \odot (\mathbf{p}\mathbf{p}^\dagger)^*$, $\mathbf{c} = \mathbf{0}$, $\ell_i = u_i = 1$, and $\mathcal{A}_i = [\underline{\theta}_i, \bar{\theta}_i]$ for $i = 1, 2, \dots, n$. In this case, all of \mathcal{A}_i in problem (CQP) are continuous sets.

■ **Virtual beamforming design [7].** Suppose that there is a set $\{1, 2, \dots, n\}$ of transmitters each equipped with a single antenna and there is a single receiver equipped with m receive antennas. Suppose that all n transmitters can fully cooperate with each other and let $\mathbf{x} \in \mathbb{C}^n$ be the virtual transmit beamforming vector formed by all transmitters. Let $\mathbf{h}_j \in \mathbb{C}^n$ be the channel vector between all transmitters and the j -th antenna of the receiver. The virtual beamforming design problem in this single-hop wireless network is to maximize the total received signal power subject to individual transmit power constraints. Mathematically, the problem can be formulated as

$$\begin{aligned} \max_{\mathbf{x} \in \mathbb{C}^n} \quad & \sum_{j=1}^m \left| \mathbf{h}_j^\dagger \mathbf{x} \right|^2 \\ \text{s.t.} \quad & |x_i| \leq \sqrt{P_i}, \quad i = 1, 2, \dots, n, \end{aligned} \quad (3)$$

where P_i is the power budget of transmitter i . Again, problem (3) is a special case of problem (CQP) with $\mathbf{Q} = -2\sum_{j=1}^m \mathbf{h}_j \mathbf{h}_j^\dagger$, $\mathbf{c} = \mathbf{0}$, $\ell_i = 0$, $u_i = \sqrt{P_i}$, $\mathcal{A}_i = [0, 2\pi]$, $i = 1, 2, \dots, n$.

III. AN ENHANCED SDR FOR PROBLEM (CQP)

In this section, we first review the conventional SDR and then develop a new enhanced SDR for problem (CQP).

A. Conventional SDR

By introducing an $n \times n$ complex matrix $\mathbf{X} = \mathbf{x}\mathbf{x}^\dagger$, problem (CQP) can be equivalently reformulated as

$$\begin{aligned} \min_{\mathbf{x}, \mathbf{X}} \quad & \frac{1}{2} \mathbf{Q} \bullet \mathbf{X} + \text{Re}(\mathbf{c}^\dagger \mathbf{x}) \\ \text{s.t.} \quad & \ell_i^2 \leq X_{ii} \leq u_i^2, \quad i = 1, 2, \dots, n, \\ & \arg(x_i) \in \mathcal{A}_i, \quad i = 1, 2, \dots, n, \\ & \mathbf{X} = \mathbf{x}\mathbf{x}^\dagger, \end{aligned} \quad (\text{P})$$

where X_{ii} is the i -th diagonal entry of \mathbf{X} . The conventional SDR of problem (P) is

$$\begin{aligned} \min_{\mathbf{x}, \mathbf{X}} \quad & \frac{1}{2} \mathbf{Q} \bullet \mathbf{X} + \text{Re}(\mathbf{c}^\dagger \mathbf{x}) \\ \text{s.t.} \quad & \ell_i^2 \leq X_{ii} \leq u_i^2, \quad i = 1, 2, \dots, n, \\ & \mathbf{X} \succeq \mathbf{x}\mathbf{x}^\dagger, \end{aligned} \quad (\text{CSDR})$$

which relaxes $\mathbf{X} = \mathbf{x}\mathbf{x}^\dagger$ to $\mathbf{X} \succeq \mathbf{x}\mathbf{x}^\dagger$ and drops the argument constraints $\arg(x_i) \in \mathcal{A}_i$ for all $i = 1, 2, \dots, n$.

The above conventional relaxation (CSDR) has been widely applied for solving problems arising from signal processing and other applications. Based on (CSDR), various (approximation) algorithms have been proposed. Indeed, all the (approximation) algorithms proposed in [3], [4], [5], [8], [10], [11], [13], [14], [19], [20], [21] are based on (CSDR) (or its equivalent reformulations).

Problem (CSDR) can be solved in polynomial time by using the interior-point algorithm (for any given positive error tolerance) [28, Sec. 6.6.3], and its optimal value serves as a lower bound of problem (P). If the optimal solution $(\bar{\mathbf{x}}, \bar{\mathbf{X}})$ of problem (CSDR) is of rank one, i.e., satisfying $\bar{\mathbf{X}} = \bar{\mathbf{x}}\bar{\mathbf{x}}^\dagger$, then $(\bar{\mathbf{x}}, \bar{\mathbf{X}})$ is the global solution of problem (P) without the argument constraints. However, $\bar{\mathbf{X}}$ might not be of rank one and $\bar{\mathbf{x}}$ might not satisfy the argument constraints. In these cases, there is a nonzero gap between problem (P) and its relaxation (CSDR), where the gap between two problems in this paper refers to the absolute value of the difference between the optimal values of the two problems.

B. An Enhanced SDR

In this subsection, we derive more valid inequalities to reduce the gap between problems (P) and (CSDR) and develop an enhanced SDR for problem (P).

Notice that the nonconvex equality constraint $\mathbf{X} = \mathbf{x}\mathbf{x}^\dagger$ in problem (P) can be equivalently reformulated as

$$\mathbf{X} \succeq \mathbf{x}\mathbf{x}^\dagger \text{ and } X_{ii} = |x_i|^2, \quad i = 1, 2, \dots, n. \quad (4)$$

In fact, if (\mathbf{x}, \mathbf{X}) satisfies (4), then $\mathbf{X} - \mathbf{x}\mathbf{x}^\dagger$ is a positive semidefinite matrix with all diagonal entries being zero, and thus $\mathbf{X} = \mathbf{x}\mathbf{x}^\dagger$. Now, we introduce the polar coordinate representation $x_i = r_i e^{j\theta_i}$ of the complex variable x_i for all $i = 1, 2, \dots, n$. By the equivalence of $\mathbf{X} = \mathbf{x}\mathbf{x}^\dagger$ and (4), we get the following proposition.

Proposition 1. *The feasible set of problem (P) can be equivalently expressed as follows: $\mathbf{X} \succeq \mathbf{x}\mathbf{x}^\dagger$ and*

$$\ell_i \leq r_i \leq u_i, \quad X_{ii} = r_i^2, \quad x_i = r_i e^{j\theta_i}, \quad \theta_i \in \mathcal{A}_i, \quad i = 1, 2, \dots, n.$$

Proof. We first show that, if $(\mathbf{x}, \mathbf{X}, \mathbf{r})$ and $\{\theta_i\}$ satisfy all conditions in the proposition, then (\mathbf{x}, \mathbf{X}) is feasible to problem (P). First, the assumption immediately implies that (\mathbf{x}, \mathbf{X}) satisfies the first two constraints in problem (P). It remains to show $\mathbf{X} = \mathbf{x}\mathbf{x}^\dagger$. This can be immediately obtained by combining $\mathbf{X} \succeq \mathbf{x}\mathbf{x}^\dagger$ and $X_{ii} = r_i^2 = |x_i|^2$, $i = 1, 2, \dots, n$. For the converse direction, assume that (\mathbf{x}, \mathbf{X}) is a feasible solution of (P). Let $r_i = |x_i|$ and $\theta_i = \arg(x_i)$ for all

$i = 1, 2, \dots, n$. Then, it is simple to check $(\mathbf{x}, \mathbf{X}, \mathbf{r})$ jointly with $\{\theta_i\}$ satisfy all conditions in the proposition. \square

The constraints $x_i = r_i e^{i\theta_i}$, $\theta_i \in \mathcal{A}_i$ and $X_{ii} = r_i^2$ in Proposition 1 are still not convex, but they allow for simple convex relaxations. Below we derive convex envelopes of these two types of nonconvex constraints, which lead to a new tighter SDR for problem (P).

Let us first consider the nonconvex set

$$\mathcal{S}_{\mathcal{A}_i} := \left\{ (x_i, r_i) \mid x_i = r_i e^{i\theta_i}, \theta_i \in \mathcal{A}_i, r_i \geq 0 \right\} \quad (5)$$

and let $\mathcal{G}_{\mathcal{A}_i}$ be its convex envelope. By using the similar arguments in [15], [29], one can show that: (1) if $\mathcal{A}_i = [\underline{\theta}_i, \bar{\theta}_i]$ with $\bar{\theta}_i - \underline{\theta}_i \leq \pi$, then

$$\mathcal{G}_{\mathcal{A}_i} = \{ (x_i, r_i) \mid |x_i| \leq r_i, \alpha_i \operatorname{Re}(x_i) + \beta_i \operatorname{Im}(x_i) \geq \gamma_i r_i \}, \quad (6)$$

where

$$\begin{aligned} \alpha_i &= \cos\left(\frac{\underline{\theta}_i + \bar{\theta}_i}{2}\right), \beta_i = \sin\left(\frac{\underline{\theta}_i + \bar{\theta}_i}{2}\right), \\ \gamma_i &= \cos\left(\frac{\underline{\theta}_i - \bar{\theta}_i}{2}\right); \end{aligned} \quad (7)$$

(2) if $\mathcal{A}_i = \{\theta_i^1, \theta_i^2, \dots, \theta_i^M\}$ is a discrete set (with a finite number of elements) with $0 \leq \theta_i^1 < \theta_i^2 < \dots < \theta_i^M < 2\pi$ and $\theta_i^{j+1} - \theta_i^j \leq \pi$ for all $i = 1, 2, \dots, M-1$, then $\mathcal{G}_{\mathcal{A}_i}$ is a polyhedral set and

$$\mathcal{G}_{\mathcal{A}_i} = \left\{ (x_i, r_i) \mid \alpha_i^j \operatorname{Re}(x_i) + \beta_i^j \operatorname{Im}(x_i) \leq \gamma_i^j r_i, j = 1, 2, \dots, M \right\}, \quad (8)$$

where

$$\begin{aligned} \alpha_i^j &= \cos\left(\frac{\theta_i^j + \theta_i^{j+1}}{2}\right), \beta_i^j = \sin\left(\frac{\theta_i^j + \theta_i^{j+1}}{2}\right), \\ \gamma_i^j &= \cos\left(\frac{\theta_i^{j+1} - \theta_i^j}{2}\right), \end{aligned}$$

and $\theta_i^{M+1} = \theta_i^1 + 2\pi$. For any $r \geq 0$, define $\mathcal{G}_{\mathcal{A}_i}(r) = \{x_i \mid (x_i, r_i) \in \mathcal{G}_{\mathcal{A}_i}, r_i = r\}$. Then, it is simple to see that $\mathcal{G}_{\mathcal{A}_i}(r)$ is a slice of $\mathcal{G}_{\mathcal{A}_i}$ with $r_i = r$ and $\mathcal{G}_{\mathcal{A}_i} = \bigcup_{r \geq 0} \{(x_i, r_i) \mid x_i \in \mathcal{G}_{\mathcal{A}_i}(r)\}$. An illustration of how $\mathcal{G}_{\mathcal{A}_i}(1)$ looks like for both continuous and discrete sets \mathcal{A}_i is given in Fig. 1.

Now, let us consider the nonconvex set

$$\{(X_{ii}, r_i) \mid X_{ii} = r_i^2, r_i \in \mathcal{B}_i\},$$

where $\mathcal{B}_i = [\ell_i, u_i]$. Let $\mathcal{F}_{\mathcal{B}_i}$ be its convex envelope. We can show that

$$\mathcal{F}_{\mathcal{B}_i} = \left\{ (X_{ii}, r_i) \mid \begin{aligned} &X_{ii} \geq r_i^2, \\ &X_{ii} - (\ell_i + u_i)r_i + \ell_i u_i \leq 0 \end{aligned} \right\}. \quad (9)$$

See Fig. 2 for an illustration of $\mathcal{F}_{\mathcal{B}_i}$.

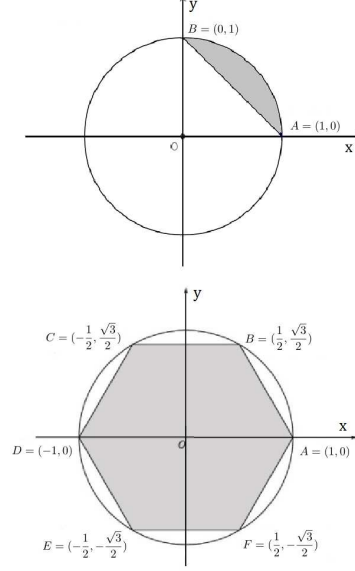


Fig. 1. An illustration of the set $\mathcal{G}_{\mathcal{A}_i}(1)$, where the top one corresponds to the continuous case where $\mathcal{A}_i = [0, \pi/2]$ and the bottom one corresponds to the discrete case where $\mathcal{A}_i = \{0, \pi/3, 2\pi/3, \pi, 4\pi/3, 5\pi/3\}$.

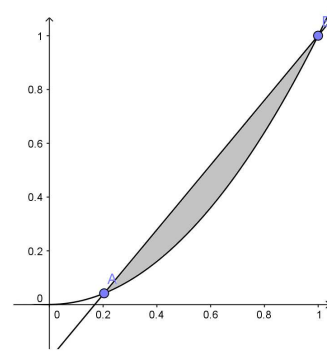


Fig. 2. An illustration of $\mathcal{F}_{\mathcal{B}_i}$ where $\mathcal{B}_i = [0.2, 1]$.

Based on the above convex envelopes of two different types of nonconvex constraints, we can obtain the following enhanced SDR for problem (P):

$$\begin{aligned} \min_{\mathbf{x}, \mathbf{X}, \mathbf{r}} \quad & \frac{1}{2} \mathbf{Q} \bullet \mathbf{X} + \operatorname{Re}(\mathbf{c}^\dagger \mathbf{x}) \\ \text{s.t.} \quad & \ell_i \leq r_i \leq u_i, \quad i = 1, 2, \dots, n, \\ & (x_i, r_i) \in \mathcal{G}_{\mathcal{A}_i}, \quad i = 1, 2, \dots, n, \\ & (X_{ii}, r_i) \in \mathcal{F}_{\mathcal{B}_i}, \quad i = 1, 2, \dots, n, \\ & \mathbf{X} \succeq \mathbf{x} \mathbf{x}^\dagger, \end{aligned} \quad (\text{ECSDR})$$

where $\mathbf{r} = [r_1, r_2, \dots, r_n]^\top$. Note that although θ_i ($i = 1, 2, \dots, n$) do not explicitly appear in problem (ECSDR), they play an important role in defining it. This is because

the sets $\mathcal{G}_{\mathcal{A}_i}$ ($i = 1, 2, \dots, n$) and thus problem (ECSDR) are determined by the range \mathcal{A}_i of θ_i . Throughout the paper, we denote

$$\mathcal{D} = \prod_{i=1}^n \mathcal{A}_i \times \prod_{i=1}^n \mathcal{B}_i$$

as the collection of \mathcal{A}_i and \mathcal{B}_i for all $i = 1, 2, \dots, n$ and denote ECSDR(\mathcal{D}) as the corresponding instance of problem (ECSDR) defined over \mathcal{D} .

Note that the constraints $(X_{ii}, r_i) \in \mathcal{F}_{\mathcal{B}_i}$ and $\ell_i \leq r_i \leq u_i$ in (ECSDR) imply $\ell_i^2 \leq X_{ii} \leq u_i^2$. Therefore, problem (ECSDR) is generally a tighter relaxation for problem (P) than (CSDR)³. First, (CSDR) completely neglects the argument constraints in problem (P) whereas the constraints $(x_i, r_i) \in \mathcal{G}_{\mathcal{A}_i}$ ($i = 1, 2, \dots, n$) in (ECSDR) carefully exploit the argument information. Moreover, the constraint $\mathbf{X} = \mathbf{x}\mathbf{x}^\dagger$ is relaxed to $\mathbf{X} \succeq \mathbf{x}\mathbf{x}^\dagger$ in (CSDR). The gap due to this relaxation is reduced in (ECSDR) because valid constraints $(X_{ii}, r_i) \in \mathcal{F}_{\mathcal{B}_i}$ ($i = 1, 2, \dots, n$) are added in (ECSDR).

C. Tightness and Relaxation Gap of (ECSDR)

In this subsection, we study the tightness and the relaxation gap of the proposed (ECSDR). We first state the following proposition.

Proposition 2. *For each $i = 1, 2, \dots, n$, if $(x_i, r_i) \in \mathcal{G}_{\mathcal{A}_i}$ and $|x_i| = r_i$, then $\arg(x_i) \in \mathcal{A}_i$.*

Instead of providing a rigorous proof for Proposition 2, we give an illustration of Proposition 2 using Fig. 1. Consider the set $\mathcal{G}_{\mathcal{A}_i}(1)$ in Fig. 1. It is simple to see from Fig. 1 that if $|x_i| = 1$, then $\arg(x_i) \in \mathcal{A}_i$.

The gap between relaxation (ECSDR) and problem (CQP) is generally nonzero. The following theorem presents a tightness result of relaxation (ECSDR).

Theorem 1. *Let $(\bar{\mathbf{x}}, \bar{\mathbf{X}}, \bar{\mathbf{r}})$ be an optimal solution of problem (ECSDR). If $|\bar{x}_i| = \bar{r}_i$ and $\bar{X}_{ii} = \bar{r}_i^2$ for all $i = 1, 2, \dots, n$, then $\bar{\mathbf{x}}$ is a global solution of problem (CQP) and thus relaxation (ECSDR) is tight.*

Proof. Let $\theta_i = \arg(\bar{x}_i)$, $i = 1, 2, \dots, n$. For each $i = 1, 2, \dots, n$, since $|\bar{x}_i| = \bar{r}_i$, it follows from Proposition 2 that $\theta_i \in \mathcal{A}_i$ and $\bar{x}_i = \bar{r}_i e^{j\theta_i}$. Furthermore, by the assumption that $\bar{X}_{ii} = \bar{r}_i^2$ for all $i = 1, 2, \dots, n$ and Proposition 1, we have that $(\bar{\mathbf{x}}, \bar{\mathbf{X}})$ is feasible to problem (P) (and in particular $\bar{\mathbf{X}} = \bar{\mathbf{x}}\bar{\mathbf{x}}^\dagger$). Therefore, $\bar{\mathbf{x}}$ is a global solution of problem (CQP) and relaxation (ECSDR) is tight. \square

In the general case, (ECSDR) might not be tight for problem (CQP). In the case that the relaxation gap is nonzero, it follows from Theorem 1 that there must exist some index $i \in \{1, 2, \dots, n\}$, such that $|\bar{x}_i| < \bar{r}_i$ and/or $\bar{X}_{ii} > \bar{r}_i^2$. Let

$$\bar{\theta}_i = \max \{\mathcal{A}_i\} \text{ and } \underline{\theta}_i := \min \{\mathcal{A}_i\}. \quad (10)$$

Next, we provide two tightness estimates of (ECSDR) in the following Proposition 3, whose proof can be found in Appendix A.

³The only case under which problems (ECSDR) and (CSDR) are equivalent is $\mathcal{A}_i = [0, 2\pi]$ for all $i = 1, 2, \dots, n$. See our discussion on this special case at the end of this section.

Proposition 3. *For a given set $\mathcal{A}_i \subseteq [\underline{\theta}_i, \bar{\theta}_i]$ with $\bar{\theta}_i - \underline{\theta}_i \leq \pi$, if $(x_i, r_i) \in \mathcal{G}_{\mathcal{A}_i}$, then*

$$r_i \geq |x_i| \geq r_i \cos \left(\frac{\bar{\theta}_i - \underline{\theta}_i}{2} \right). \quad (11)$$

for a given set $\mathcal{B}_i = [\ell_i, u_i]$, if $(X_{ii}, r_i) \in \mathcal{F}_{\mathcal{B}_i}$, then

$$0 \leq X_{ii} - r_i^2 \leq \frac{(u_i - \ell_i)^2}{4}. \quad (12)$$

Define the width of \mathcal{A}_i as

$$\omega(\mathcal{A}_i) := \bar{\theta}_i - \underline{\theta}_i, \quad (13)$$

where $\bar{\theta}_i$ and $\underline{\theta}_i$ are defined in (10), and the width of \mathcal{B}_i as

$$\omega(\mathcal{B}_i) := u_i - \ell_i. \quad (14)$$

We can see from Proposition 3 that: (1) when $\omega(\mathcal{A}_i)$ becomes close to zero, $|x_i|$ will be close to r_i and the constraint $(x_i, r_i) \in \mathcal{G}_{\mathcal{A}_i}$ will be very effective in reducing the difference between r_i and $|x_i|$; (2) similarly, when $\omega(\mathcal{B}_i)$ becomes close to zero, X_{ii} will be close to r_i^2 and the constraint $(X_{ii}, r_i) \in \mathcal{F}_{\mathcal{B}_i}$ will be very effective in reducing the difference between X_{ii} and r_i^2 .

Now let us discuss two very special cases of (ECSDR). The first case is $\ell_i = u_i = 1$ for all $i = 1, 2, \dots, n$. In this case, the set $\mathcal{F}_{\mathcal{B}_i}$ reduces $\mathcal{F}_{\mathcal{B}_i} = \{(X_{ii}, r_i) \mid X_{ii} = 1, r_i = 1\}$ and thus the constraint $X_{ii} = r_i^2$ is always satisfied. Hence, if the gap between problem (CQP) and its relaxation (ECSDR) is nonzero, then the gap must be due to the convex relaxation $(x_i, r_i) \in \mathcal{G}_{\mathcal{A}_i}$, i.e., there must exist some $i \in \{1, 2, \dots, n\}$ such that $r_i > |x_i|$. This special case has been studied in [15], [23]. This paper studies a more general problem (CQP) (with interval modulus constraints) and can be regarded as a nontrivial extension from the unit-modulus case in [15], [23]. Note that it is straightforward to obtain an SDR for the unit-modulus problem while it is not easy to obtain the SDR for problem (CQP), as the latter requires the use of the polar coordinate representation of the complex variables and Proposition 1. The second case is $\mathcal{A}_i = [0, 2\pi]$ for all $i = 1, 2, \dots, n$. In this case, we can show that (ECSDR) is equivalent to (CSDR). To be more specific, the constraints $(x_i, r_i) \in \mathcal{G}_{\mathcal{A}_i}$ and $(X_{ii}, r_i) \in \mathcal{F}_{\mathcal{B}_i}$ in this case become

$$r_i \geq |x_i|, X_{ii} \geq r_i^2, X_{ii} - (\ell_i + u_i)r_i + \ell_i u_i \leq 0.$$

Then, for any feasible solution (\mathbf{x}, \mathbf{X}) of (CSDR), we can set $r_i = \sqrt{X_{ii}}$ for $i = 1, 2, \dots, n$ and check that $(\mathbf{x}, \mathbf{X}, \mathbf{r})$ is a feasible solution of (ECSDR). Therefore, the two relaxations (ECSDR) and (CSDR) are equivalent in this case⁴. Except this special case, (ECSDR) is tighter than (CSDR) as discussed before and as will be illustrated later in Section V.

⁴Although relaxation (ECSDR) is not tighter than (CSDR) in this special case, (ECSDR) still plays an important role of generating the lower bounds in the ECSDR-BB algorithm in the next section, where as the set \mathcal{A}_i is recursively partitioned into smaller subsets, the quality of relaxation (ECSDR) defined over the subsets will become better than that of (CSDR).

IV. PROPOSED GLOBAL BRANCH-AND-BOUND ALGORITHM

In this section, we propose a global branch-and-bound algorithm based on the enhanced relaxation (ECSDR) for solving problem (CQP) (equivalent to problem (P)). A typical branch-and-bound algorithm (for a minimization problem) is generally based on an enumeration procedure, which partitions the feasible region to smaller subregions and constructs subproblems over the partitioned subregions recursively. In the enumeration procedure, a lower bound for each subproblem is estimated by solving a relaxation problem. Meanwhile, an upper bound is obtained from the best known feasible solution generated by the enumeration procedure or by some other local optimization/heuristic algorithms. The procedure terminates until the difference between the upper bound and the lower bound is smaller than the given error tolerance $\epsilon > 0$, and then an ϵ -optimal solution (defined as below) can be obtained.

Definition 1 (ϵ -Optimal Solution). *Given any $\epsilon > 0$, a feasible point \mathbf{x} is called an ϵ -optimal solution of problem (CQP) if it satisfies $F(\mathbf{x}) - \nu^* \leq \epsilon$.*

In the remaining part of this section, we first present our proposed branch-and-bound algorithm for solving problem (CQP) in Section III-A. Then, we show that our proposed branch-and-bound algorithm indeed can find an ϵ -optimal solution of problem (CQP) (for any given $\epsilon > 0$) and analyze its worst-case iteration complexity in Section III-B.

A. Proposed Algorithm

To develop a branch-and-bound algorithm for solving problem (CQP), let us first recall Theorem 1. Theorem 1 shows that, if the gap between problem (CQP) and its corresponding relaxation (ECSDR) is not zero, then there must exist some $i \in \{1, 2, \dots, n\}$ with $|\bar{x}_i| < \bar{r}_i$ and/or $\bar{X}_{ii} > \bar{r}_i^2$. Moreover, Proposition 3 further shows that we can partition the sets \mathcal{A}_i and \mathcal{B}_i to reduce the difference $\bar{r}_i - |\bar{x}_i|$ and $\bar{X}_{ii} - \bar{r}_i^2$, respectively. Based on the above observations, we are now ready to present the main steps of the branch-and-bound algorithm. For ease of presentation, we introduce the following notations. Let $\mathcal{D}^0 = \prod_{i=1}^n \mathcal{A}_i^0 \times \prod_{i=1}^n \mathcal{B}_i^0$ with $\mathcal{A}_i^0 = \mathcal{A}_i$ and $\mathcal{B}_i = [\ell_i, u_i]$ be the initial feasible set of the polar coordinate variables $\{\theta_i\}$ and \mathbf{r} , and $\mathcal{D}^k = \prod_{i=1}^n \mathcal{A}_i^k \times \prod_{i=1}^n \mathcal{B}_i^k \subseteq \mathcal{D}^0$ be a partitioned subset indexed by k .

Lower Bound. In the branch-and-bound algorithm, the initial feasible set \mathcal{D}^0 will be recursively partitioned into smaller subsets. Obviously, the optimal value L^k of the relaxation problem $\text{ECSDR}(\mathcal{D}^k)$ is a lower bound of the optimal value of problem (CQP) defined over the subset \mathcal{D}^k . Therefore, the smallest lower bound among all bounds is a lower bound of the optimal value of the original problem (CQP). This statement will be formally summarized in Theorem 2.

Upper Bound. An upper bound of problem (CQP) can be obtained by appropriately scaling the solution of any relaxation problem. More specifically, we solve a relaxation (ECSDR) (defined over a partitioned subset) to obtain its optimal so-

lution $(\bar{\mathbf{x}}, \bar{\mathbf{X}}, \bar{\mathbf{r}})$. Then, we generate a feasible solution of problem (CQP) by using the following scaling operation

$$\hat{\mathbf{x}} = \text{Scale}(\bar{\mathbf{x}}, \bar{\mathbf{r}}) := \left[\bar{r}_1 e^{i\hat{\theta}_1}, \dots, \bar{r}_n e^{i\hat{\theta}_n} \right]^T, \quad (15)$$

where

$$\hat{\theta}_i \in \arg \min_{\theta \in \mathcal{A}_i} \min \{ |\theta_i - \arg(\bar{x}_i)|, 2\pi - |\theta_i - \arg(\bar{x}_i)| \}$$

and \mathcal{A}_i is normalized to satisfy $\mathcal{A}_i \subseteq (-\pi, \pi]$. If the optimal solution to the above problem is not unique, then we just pick one solution. It is simple to check that the above $\hat{\mathbf{x}}$ is feasible to problem (CQP). Consequently, $F(\hat{\mathbf{x}})$ is an upper bound of problem (CQP). In our branch-and-bound algorithm, we use U^* to denote the best upper bound during the enumeration procedure (i.e., the smallest objective values at all of known feasible solutions at the current iteration) and use x^* to denote the solution that achieves the smallest upper bound.

In the proposed branch-and-bound algorithm, we construct a so-called node for each subproblem. The node is denoted as $\{\mathcal{D}^k, \mathbf{x}^k, \mathbf{X}^k, \mathbf{r}^k, \hat{\mathbf{x}}^k, L^k\}$, in which \mathcal{D}^k is the partitioned subset of the subproblem, $(\mathbf{x}^k, \mathbf{X}^k, \mathbf{r}^k)$ and L^k are the optimal solution and the optimal value of problem $\text{ECSDR}(\mathcal{D}^k)$, and $\hat{\mathbf{x}}^k = \text{Scale}(\mathbf{x}^k, \mathbf{r}^k)$ (with the operator $\text{Scale}(\cdot, \cdot)$ being defined in (15)).

Termination Criterion. If

$$U^* - L^k \leq \epsilon \quad (16)$$

at iteration k , where ϵ is the preselected error tolerance, we terminate the algorithm; otherwise we select a node and branch the feasible set of a variable according to some rule. We can see from (16) that, both lower and upper bounds are important to avoid unnecessary branches and enumerations and good lower and upper bounds can significantly improve the computational efficiency of our proposed algorithm. Below, we shall introduce our node selection and branching rules one by one.

Node Selection Rule. For node k , if its lower bound L^k is larger than the upper bound U^* , then the global solution of the original problem cannot be located in the set associated with this node. We call a node as an *active* node if its lower bound is smaller than the best known upper bound. Therefore, all of the inactive nodes will not be enumerated in the branch-and-bound algorithm. Let us use \mathcal{P} to denote the set of all active nodes. Our selection rule is to select the active node with the smallest lower bound from \mathcal{P} (to be branched) at each iteration.

Branching Rule. Let $\{\mathcal{D}^k, \mathbf{x}^k, \mathbf{X}^k, \mathbf{r}^k, \hat{\mathbf{x}}^k, L^k\}$ be the selected node that has the smallest lower bound in \mathcal{P} and let

$$\begin{aligned} i_1^* &= \arg \max_i \{ |\hat{x}_i^k - x_i^k| \}, \\ S_1^* &= \max_i \{ |\hat{x}_i^k - x_i^k| \}, \\ i_2^* &= \arg \max_i \{ X_{ii}^k - (r_i^k)^2 \}, \\ S_2^* &= \max_i \{ X_{ii}^k - (r_i^k)^2 \}. \end{aligned} \quad (17)$$

The quantity $\max\{S_1^*, S_2^*\}$ somehow measures the gap of the corresponding relaxation (ECSDR). If $S_1^* \geq S_2^*$, then we select $\mathcal{A}_{i_1^*}^k$ to branch; otherwise we select $\mathcal{B}_{i_2^*}^k$ to branch. The selected

set is branched into two subsets by the following rule: if the selected set is an interval, then we partition it into two sub-intervals with equal lengths; if the selected set is a finite set (in the case where $S_1^* \geq S_2^*$ and $\mathcal{A}_{i_1^*}^k$ is a finite set), then we partition the set into two subsets

$$\left\{ \theta \mid \theta \in \mathcal{A}_{i_1^*}^k, \theta \leq \theta_{i_1^*}^k \right\} \text{ and } \left\{ \theta \mid \theta \in \mathcal{A}_{i_1^*}^k, \theta > \theta_{i_1^*}^k \right\},$$

where

$$\theta_{i_1^*}^k = \frac{1}{2} \left(\min \left\{ \mathcal{A}_{i_1^*}^k \right\} + \max \left\{ \mathcal{A}_{i_1^*}^k \right\} \right).$$

Based on the above rules, we branch the set \mathcal{D}^k into two new sets (denoted as \mathcal{D}_-^k and \mathcal{D}_+^k). It follows from Proposition 3 that the corresponding relaxation problems defined over the newly obtained two sets \mathcal{D}_-^k and \mathcal{D}_+^k , i.e., the two children problems, are tighter than the one defined over the original set \mathcal{D}^k . Once \mathcal{D}^k has been branched into two sets, the problem instance defined over it will be deleted from the problem list \mathcal{P} and the two children problems will be added into \mathcal{P} if their lower bounds are less than or equal to the current best upper bound.

By judiciously combining the above main steps, we can obtain our proposed branch-and-bound algorithm for solving problem (CQP) (equivalent to problem (P)). The pseudocodes of our proposed algorithm are given in Algorithm 1. We will call the algorithm ECSDR-BB (Enhanced Complex SemiDefinite Relaxation based Branch-and-Bound) for short.

B. Global Convergence and Worst-Case Iteration Complexity

In this subsection, we present some theoretical results of our proposed ECSDR-BB algorithm.

The following Theorem 2 shows that the sequence $\{L^k\}$ generated by the ECSDR-BB algorithm is a lower bound of the optimal value of problem (CQP) and the solution \mathbf{x}^* returned by the algorithm is an ϵ -optimal solution of the problem. The proof of the theorem can be found in Appendix B.

Theorem 2. *Let $\{\mathcal{D}^k, \mathbf{x}^k, \mathbf{X}^k, \mathbf{r}^k, \hat{\mathbf{x}}^k, L^k\}$ be the node selected in Line 9 of the ECSDR-BB algorithm. Then we have*

$$L^k \leq \nu^* \leq F(\hat{\mathbf{x}}^k). \quad (18)$$

Moreover, if (16) holds true, then \mathbf{x}^* returned by the algorithm is an ϵ -optimal solution of problem (CQP).

Next, we will estimate $F(\hat{\mathbf{x}}^k) - L^k$ and show that (16) will be satisfied after a finite number of iterations. Define

$$u_{\max} = \max\{u_1, u_2, \dots, u_n\} \quad (19)$$

and the bounded set

$$\mathcal{X} = \{\mathbf{x} \mid |x_i| \leq u_{\max}, i = 1, 2, \dots, n\}. \quad (20)$$

Since $F(\mathbf{x})$ is uniformly continuous over the bounded set \mathcal{X} , there must exist a constant $M_F > 0$ such that

$$|F(\mathbf{x}) - F(\mathbf{x}')| \leq M_F \|\mathbf{x} - \mathbf{x}'\|_2, \forall \mathbf{x}, \mathbf{x}' \in \mathcal{X}. \quad (21)$$

The next lemma gives an upper bound on $F(\hat{\mathbf{x}}^k) - L^k$, whose proof is relegated to Appendix C.

Algorithm 1: ECSDR-BB Algorithm for Solving Problem (CQP)

- 1: **input:** An instance of problem (CQP) and an error tolerance $\epsilon > 0$.
- 2: Initialize $\mathcal{P} = \emptyset$, $\mathcal{D}^0 = \prod_{i=1}^n \mathcal{A}_i^0 \times \prod_{i=1}^n \mathcal{B}_i^0 := \prod_{i=1}^n \mathcal{A}_i \times \prod_{i=1}^n [\ell_i, u_i]$, and set $k = 0$. // Initialization.
- 3: Solve ECSDR(\mathcal{D}^0) for its optimal solution $(\mathbf{x}^0, \mathbf{X}^0, \mathbf{r}^0)$ and its optimal value L^0 . // Solve relaxation (ECSDR) at the root node.
- 4: Compute the feasible point $\hat{\mathbf{x}}^0 = \text{Scale}(\mathbf{x}^0, \mathbf{r}^0)$.
- 5: Set $U^* = F(\hat{\mathbf{x}}^0)$ and $\mathbf{x}^* = \hat{\mathbf{x}}^0$. // Initial Upper Bound and Optimal Solution.
- 6: Add $\{\mathcal{D}^0, \mathbf{x}^0, \mathbf{X}^0, \mathbf{r}^0, \hat{\mathbf{x}}^0, L^0\}$ into the node list \mathcal{P} .
- 7: **loop**
- 8: Set $k \leftarrow k + 1$.
- 9: Using the **Node Selection Rule** to choose a problem from \mathcal{P} , denoted as $\{\mathcal{D}^k, \mathbf{x}^k, \mathbf{X}^k, \mathbf{r}^k, \hat{\mathbf{x}}^k, L^k\}$, such that L^k is the smallest one in \mathcal{P} . // Lower Bound.
- 10: Delete the chosen node from \mathcal{P} .
- 11: **if** $U^* - L^k \leq \epsilon$ **then**
- 12: return \mathbf{x}^* and U^* and terminate the algorithm. // Terminate if (16) is satisfied.
- 13: **end if**
- 14: Choose the set according to (17) and branch \mathcal{D}^k into two subsets \mathcal{D}_-^k and \mathcal{D}_+^k by using the **Branching Rule**. // Branch.
- 15: **for** $s \in \{-, +\}$ **do**
- 16: Solve ECSDR(\mathcal{D}_s^k) for its solution $(\mathbf{x}_s^k, \mathbf{X}_s^k, \mathbf{r}_s^k)$ and its optimal value L_s^k . // Solve the children problems.
- 17: Compute the feasible point $\hat{\mathbf{x}}_s^k = \text{Scale}(\mathbf{x}_s^k, \mathbf{r}_s^k)$.
- 18: **if** $U^* > F(\hat{\mathbf{x}}_s^k)$ **then**
- 19: set $U^* = F(\hat{\mathbf{x}}_s^k)$, $\mathbf{x}^* = \hat{\mathbf{x}}_s^k$. // Update Upper Bound and Optimal Solution.
- 20: **end if**
- 21: **if** $L_s^k < U^*$ **then**
- 22: add $\{\mathcal{D}_s^k, \mathbf{x}_s^k, \mathbf{X}_s^k, \mathbf{r}_s^k, \hat{\mathbf{x}}_s^k, L_s^k\}$ into \mathcal{P} .
- 23: **end if**
- 24: **end for**
- 25: **end loop**

Lemma 1. *Let*

$$M_1 = \sqrt{n}M_F + n^{\frac{3}{2}}u_{\max} \|\mathbf{Q}\|_F \quad (22)$$

and

$$M_2 = \frac{1}{2}n^{\frac{3}{2}} \|\mathbf{Q}\|_F, \quad (23)$$

where M_F is given in (21). Then, we have

$$F(\hat{\mathbf{x}}^k) - L^k \leq M_1 S_1^* + M_2 S_2^*, \quad (24)$$

where S_1^* and S_2^* are defined in (17).

Based on Lemma 1, we can show the following result and we relegate its proof to Appendix D.

Lemma 2. *Let*

$$\kappa_1 = \left[\frac{8\epsilon}{u_{\max}(M_1 + M_2)} \right]^{\frac{1}{2}} \quad (25)$$

and

$$\kappa_2 = \left[\frac{4\epsilon}{M_1 + M_2} \right]^{\frac{1}{2}}, \quad (26)$$

where M_1 and M_2 are defined in (22) and (23), respectively. If one of the following three conditions is satisfied:

(C1) $S_1^* \geq S_2^*$, $\mathcal{A}_{i_1}^k = [\underline{\theta}_{i_1}^k, \bar{\theta}_{i_1}^k]$, and $\bar{\theta}_{i_1}^k - \underline{\theta}_{i_1}^k \leq \min\{\kappa_1, \pi\}$,
 (C2) $S_1^* \geq S_2^*$, and $\mathcal{A}_{i_1}^k$ is a singleton,
 (C3) $S_1^* < S_2^*$, $\mathcal{B}_{i_2}^k = [\ell_{i_2}^k, u_{i_2}^k]$, and $u_{i_2}^k - \ell_{i_2}^k \leq \kappa_2$,
 then (16) is satisfied and thus the ECSDR-BB algorithm terminates in Line 12.

Based on the above two lemmas, we obtain the main result of this subsection, which shows that the ECSDR-BB algorithm will terminate within a finite number of iterations in (27).

Theorem 3. For any given error tolerance $\epsilon > 0$ and any given instance of problem (CQP), the ECSDR-BB algorithm will return an ϵ -optimal solution of the given instance within at most

$$K := \prod_{i=1}^n \left[\mu(\mathcal{A}_i) \times \max \left\{ \left\lceil \frac{2\omega(\mathcal{B}_i)}{\kappa_2} \right\rceil, 1 \right\} \right] \quad (27)$$

iterations, where

$$\mu(\mathcal{A}_i) = \begin{cases} \max \left\{ \left\lceil \frac{2\omega(\mathcal{A}_i)}{\min\{\kappa_1, \pi\}} \right\rceil, 1 \right\}, & \text{if } \mathcal{A}_i \text{ is an interval;} \\ |\mathcal{A}_i|, & \text{if } \mathcal{A}_i \text{ is a finitely discrete set,} \end{cases} \quad (28)$$

and κ_1 and κ_2 are the constants defined in (25) and (26), respectively.

The proof of Theorem 3 can be found in Appendix E. Two remarks on Theorem 3 are in order. First, from Theorem 3, we can obtain the global convergence of the ECSDR-BB algorithm, i.e., both the sequences of the upper bounds and the lower bounds generated by the algorithm with $\epsilon = 0$ converge to the optimal value of problem (CQP). In practice, we need to preselect a positive error tolerance ϵ in our proposed algorithm, as in most of iterative optimization algorithms. Second, Theorem 3 shows that the total number of iterations K in (27) for the ECSDR-BB algorithm to return an ϵ -optimal solution of problem (CQP) is exponential with respect to the number of variables n . The iteration complexity of our proposed algorithm seems high at first sight. However, as will be shown in Section V, its practical number of iterations is actually significantly less than the worst-case bound in (27). It is also worth remarking that there is no polynomial time algorithm which can globally solve the problem (unless $P=NP$), because the problem is NP-hard.

V. NUMERICAL SIMULATIONS

In this section, we present some numerical simulation results to demonstrate the tightness of our proposed relaxation (ECSDR) and the efficiency of our proposed ECSDR-BB algorithm for problem (CQP). We apply the ECSDR-BB algorithm to solve three optimization problems arising from signal processing applications introduced in Section II, i.e., the MIMO detection problem (1), the unimodular radar code design problem (2), and the virtual beamforming design problem (3). All of these three problems are special cases of problem (CQP) but they have different characteristics, e.g., the MIMO detection problem has discrete argument constraints and unit-modulus constraints; the unimodular radar code design problem has

continuous argument constraints (but not equal $[0, 2\pi]$) and unit-modulus constraints; and the virtual beamforming design problem has continue argument constraints (and equal $[0, 2\pi]$) and interval modulus constraints. All of the experiments are implemented in MATLAB, with SeDuMi [30] being used to solve semidefinite programs (SDPs). All the algorithms are run on a PC with Intel Core i7-2600 (3.40GHz) and 4GB memory. In all experiments, the error tolerance of the proposed ECSDR-BB algorithm is set to be $\epsilon = 10^{-4}$.

A. Numerical Results of MIMO Detection

We generate the instances of the MIMO detection problem (1) as in [26], [27]: we first generate \mathbf{H} according to the standard complex Gaussian distribution; then we generate a complex vector \mathbf{x}^* with $|x_i^*| = 1$ and $\arg(x_i^*)$ being uniformly chosen from the discrete set \mathcal{A}_i for all $i = 1, 2, \dots, n$; finally we set $\mathbf{r} = \mathbf{H}\mathbf{x}^* + \sigma\mathbf{v}$, where $\mathbf{v} \in \mathbb{C}^n$ is a Gaussian noise obeying the standard complex Gaussian distribution and σ is a parameter which controls the SNR determined by $\text{SNR} = 10 \log_{10} (\|\mathbf{H}\mathbf{x}^*\|_2^2 / \sigma^2 n)$. In our simulations, \mathcal{A}_i is either $\{0, \pi/2, \pi, 3\pi/2\}$ (i.e., QPSK) or $\{0, \pi/4, \pi/2, 3\pi/4, \pi, 5\pi/4, 3\pi/2, 7\pi/4\}$ (i.e., 8-PSK).

For each setup, we generate 50 problem instances and apply our proposed algorithm (i.e., Algorithm 1) to solve them. All results in this subsection are obtained by averaging over the 50 generated instances. Numerical results are summarized in Tables I and II, where “ObjVal” denotes the objective value returned by the proposed ECSDR-BB algorithm; “LBdE” and “LBdC” denote the lower bounds (i.e., the optimal objective values) returned by two relaxations (ECSDR) and (CSDR) (for problem (1)), respectively; “CldGap” denotes $(\text{LBdE} - \text{LBdC}) / (\text{ObjVal} - \text{LBdC}) \times 100\%$, which measures how much of the gap in (CSDR) is closed by (ECSDR); “Time” and “# Iter” denote the CPU time and the number of iterations of the ECSDR-BB algorithm for solving problem (CQP); and “TimeE” and “TimeC” denote the CPU time of solving relaxations (ECSDR) and (CSDR), respectively. Notice that “CldGap” defined in the above must be in $[0, 1]$ due to the fact $\text{ObjVal} \geq \text{LBdE} \geq \text{LBdC}$.

We first compare the two relaxations (ECSDR) and (CSDR) in terms of their tightness and computational efficiency. We can see from Table I that relaxation (ECSDR) is generally much tighter than (CSDR). In particular, in cases of $M = 4$ and $\text{SNR} = 25$, our proposed relaxation (ECSDR) is exact, i.e., the optimal solution and the optimal objective value of relaxation (ECSDR) are equal to that of the original problem; in cases of $\text{SNR} \geq 15$, our proposed relaxation (ECSDR) narrows down over 50% of the gap due to (CSDR); and in all cases, LBdE is generally larger than LBdC and more than 30% of the gap in (CSDR) is closed by (ECSDR). These results clearly show that the new envelope constraints added in (ECSDR) (as compared to (CSDR)) are indeed very useful to reduce the relaxation gap of (CSDR). From Table II, we can observe that the two relaxations have similar computational efficiency. In fact, since the number of constraints in (ECSDR) is larger than that of (CSDR), the CPU time of solving (ECSDR) is generally larger than that of solving (CSDR). However, the

TABLE I
OBJECTIVE VALUES AND LOWER BOUNDS OF MIMO DETECTION
PROBLEM (1)

(m, n, M)	SNR	ObjVal	LBdE	LBdC	CldGap
(15, 10, 4)	25	0.954	0.954	0.662	100.0 %
(15, 10, 4)	20	3.118	3.102	2.124	98.4 %
(15, 10, 4)	15	9.809	9.575	6.395	93.1 %
(15, 10, 4)	10	30.093	28.064	21.124	77.4 %
(15, 10, 4)	5	85.843	72.824	56.006	56.4 %
(15, 10, 8)	25	0.960	0.953	0.669	97.6 %
(15, 10, 8)	20	3.082	2.972	2.034	89.6 %
(15, 10, 8)	15	9.712	8.678	6.605	66.7 %
(15, 10, 8)	10	28.858	24.333	20.351	46.8 %
(15, 10, 8)	5	78.708	71.169	65.251	44.0 %
(30, 20, 4)	25	3.638	3.638	2.366	100.0 %
(30, 20, 4)	20	12.489	12.464	8.376	99.4 %
(30, 20, 4)	15	38.064	36.335	24.977	86.8 %
(30, 20, 4)	10	119.411	106.786	79.083	68.7 %
(30, 20, 4)	5	348.242	288.539	229.577	49.7 %
(30, 20, 8)	25	3.851	3.764	2.544	93.3 %
(30, 20, 8)	20	11.765	11.084	7.783	82.9 %
(30, 20, 8)	15	37.940	32.936	26.065	57.9 %
(30, 20, 8)	10	115.252	91.510	78.141	36.0 %
(30, 20, 8)	5	285.485	252.054	236.121	32.3 %

TABLE II
CPU TIME (IN SECONDS) AND NUMBER OF ITERATIONS FOR SOLVING
MIMO DETECTION PROBLEM (1)

(m, n, M)	SNR	# Iter	Time	TimeE	TimeC
(15, 10, 4)	25	1.0	0.09	0.09	0.07
(15, 10, 4)	20	1.3	0.14	0.09	0.07
(15, 10, 4)	15	2.3	0.29	0.08	0.07
(15, 10, 4)	10	3.8	0.53	0.08	0.07
(15, 10, 4)	5	9.8	1.36	0.07	0.07
(15, 10, 8)	25	1.6	0.23	0.11	0.07
(15, 10, 8)	20	3.1	0.47	0.10	0.07
(15, 10, 8)	15	6.5	1.04	0.09	0.07
(15, 10, 8)	10	13.3	2.08	0.09	0.07
(15, 10, 8)	5	23.1	3.49	0.08	0.06
(30, 20, 4)	25	1.0	0.18	0.18	0.12
(30, 20, 4)	20	1.4	0.30	0.18	0.12
(30, 20, 4)	15	4.0	1.03	0.15	0.12
(30, 20, 4)	10	8.2	2.14	0.15	0.12
(30, 20, 4)	5	40.1	9.25	0.13	0.11
(30, 20, 8)	25	3.1	0.96	0.19	0.12
(30, 20, 8)	20	7.3	2.32	0.18	0.11
(30, 20, 8)	15	15.2	4.72	0.18	0.12
(30, 20, 8)	10	77.8	21.02	0.15	0.11
(30, 20, 8)	5	161.3	42.36	0.15	0.11

CPU time of solving (ECSDR) is not much larger than that of solving (CSDR). This is because the constraints added in (ECSDR) (compared to (CSDR)) are all “simple” linear constraints. Based on the above analysis and numerical results, we conclude that (ECSDR) generally is much tighter than (CSDR) but solving (ECSDR) takes only slightly more CPU time than solving (CSDR).

We can also see from Table II that our proposed ECSDR-BB algorithm can solve all problem instances within 162 iterations and within 43 seconds (on average). These results show that our proposed ECSDR-BB algorithm is very efficient for globally solving the MIMO detection problem. We will further compare the efficiency of our proposed ECSDR-BB

TABLE III
OBJECTIVE VALUES AND UPPER BOUNDS OF UNIMODULAR RADAR CODE
DESIGN PROBLEM (2)

ID	$\omega(\mathcal{A}_i)$	ObjVal	UBdE	UBdC	CldGap
1	$\pi/3$	73.76	74.47	140.93	99.0%
2	$\pi/3$	11.74	11.88	14.63	95.0%
3	$\pi/3$	10.73	10.88	13.97	95.3%
4	$\pi/3$	10.55	10.67	14.00	96.4%
5	$\pi/3$	12.23	12.24	14.06	99.4%
6	$2\pi/3$	20.55	22.12	24.13	56.1%
7	$2\pi/3$	35.02	40.41	48.88	61.1%
8	$2\pi/3$	12.30	12.94	13.76	56.0%
9	$2\pi/3$	16.91	17.59	19.09	68.8%
10	$2\pi/3$	22.00	23.11	25.02	63.1%

TABLE IV
CPU TIME (IN SECONDS) AND NUMBER OF ITERATIONS FOR SOLVING
UNIMODULAR RADAR CODE DESIGN PROBLEM (2)

ID	$\omega(\mathcal{A}_i)$	# Iter	Time	TimeE	TimeC
1	$\pi/3$	19	2.09	0.05	0.03
2	$\pi/3$	12	1.17	0.05	0.04
3	$\pi/3$	11	1.07	0.05	0.04
4	$\pi/3$	6	0.53	0.05	0.03
5	$\pi/3$	2	0.15	0.05	0.04
6	$2\pi/3$	24	2.45	0.05	0.03
7	$2\pi/3$	8	0.78	0.05	0.04
8	$2\pi/3$	20	1.93	0.05	0.03
9	$2\pi/3$	9	0.83	0.05	0.03
10	$2\pi/3$	11	1.06	0.05	0.04

algorithm with a specially designed algorithm for solving the MIMO detection problem in Section IV-D.

B. Numerical Results of Unimodular Radar Code Design

We generate the instances of the unimodular radar code design problem (2) as in [4]: we set each entry of \mathbf{M} to be $M_{ij} = \rho^{|i-j|}$ with $\rho \in [0.2, 0.8]$; set $N = 7$ and $\mathbf{x}^0 = [1, 1, 1, -1, -1, 1, -1]^T$ (i.e., the Barker code of length 7); set the steering vector $\mathbf{p} = [1, e^{i2\pi f_d T_r}, \dots, e^{i2\pi(N-1)f_d T_r}]^T$ with $f_d T_r = 0.15$; and set the similarity tolerance δ in (2) such that $\arccos(1 - \delta^2/2)$ is equal to either $\pi/6$ or $\pi/3$.

For each value of the parameter δ , we generate 5 problem instances and apply our proposed algorithm (i.e., Algorithm 1) to solve them. Numerical results on all 10 problem instances are summarized in Tables III and IV, where “ID” denotes the IDs of the corresponding problem instances, $\omega(\mathcal{A}_i)$ denotes the width of set \mathcal{A}_i (cf. (13)), “UBdE” and “UBdC” denote the upper bounds⁵ (i.e., the optimal objective values) returned by two relaxations (ECSDR) and (CSDR) (for problem (2)), respectively, “CldGap” denotes $(\text{UBdC} - \text{UBdE})/(\text{UBdC} - \text{ObjVal}) \times 100\%$, and all the others have the same meanings as that in Tables I and II. By the definition of $\omega(\mathcal{A}_i)$ (cf. (13)), we have $\omega(\mathcal{A}_i) = \pi/3$ if $\arccos(1 - \delta^2/2) = \pi/6$ and $\omega(\mathcal{A}_i) = 2\pi/3$ if $\arccos(1 - \delta^2/2) = \pi/3$.

We can observe and conclude from the results listed in Tables III and IV that:

⁵Recall that problem (2) is a maximization problem and thus the optimal values of the corresponding relaxations are upper bounds of its optimal value.

TABLE V
OBJECTIVE VALUES AND UPPER BOUNDS OF VIRTUAL BEAMFORMING
DESIGN PROBLEM (3)

(m, n)	ObjVal	UBdE	UBdC
(5, 5)	108.837	108.858	108.858
(10, 5)	187.625	187.647	187.647
(15, 5)	259.929	260.127	260.127
(5, 10)	364.247	364.746	364.746
(10, 10)	534.053	535.807	535.807
(15, 10)	701.893	703.075	703.075
(5, 15)	696.457	699.092	699.092
(10, 15)	1030.088	1037.109	1037.109
(15, 15)	1320.666	1327.523	1327.523
(5, 20)	1154.460	1163.583	1163.583
(10, 20)	1619.981	1633.517	1633.517
(15, 20)	2039.053	2057.837	2057.837

TABLE VI
CPU TIME (IN SECONDS) AND NUMBER OF ITERATIONS FOR SOLVING
VIRTUAL BEAMFORMING DESIGN PROBLEM (3)

(m, n)	# Iter	Time	TimeE	TimeC
(5, 5)	1.6	0.19	0.06	0.06
(10, 5)	1.5	0.17	0.06	0.06
(15, 5)	3.1	0.45	0.06	0.06
(5, 10)	11.4	3.01	0.06	0.06
(10, 10)	20.6	5.68	0.06	0.06
(15, 10)	14.4	3.89	0.06	0.06
(5, 15)	94.2	38.92	0.06	0.06
(10, 15)	157.1	58.51	0.06	0.06
(15, 15)	161.4	58.25	0.06	0.06
(5, 20)	601.4	267.86	0.06	0.06
(10, 20)	534.8	237.52	0.06	0.06
(15, 20)	541.7	242.19	0.06	0.06

- 1) (ECSDR) is generally much tighter than (CSDR), especially when $\omega(\mathcal{A}_i)$ is small. This is consistent with the analysis in Proposition 3: since $r_i = 1$ in the unimodular radar code design problem (2), then the inequality in (11) reduces to $1 \geq |x_i| \geq \cos(\omega(\mathcal{A}_i)/2)$, which shows that a smaller $\omega(\mathcal{A}_i)$ generally leads to a smaller gap $1 - |x_i|$.
- 2) Solving (ECSDR) takes slightly more CPU time than solving (CSDR).
- 3) Our proposed ECSDR-BB algorithm is able to efficiently solve all generated problem instances within satisfactory computational time (i.e., less than 3 seconds) and within a relatively small number of iterations (i.e., less than 24 iterations).

C. Numerical Results of Virtual Beamforming Design

We generate the instances of the virtual beamforming design problem (3): we set $P_i = 1$ for all $i = 1, 2, \dots, n$ and generate \mathbf{h}_j for all $j = 1, 2, \dots, m$ according to the standard complex Gaussian distribution (as in [12, Section 4.3.5]). In our simulations, we set $m \in \{5, 10, 15\}$ and $n \in \{5, 10, 15, 20\}$ (and thus there are in total 12 different pairs of (m, n)). For each pair of (m, n) , we generate 50 instances and apply our proposed ECSDR-BB algorithm to solve them. All results in this subsection are obtained by averaging over the 50 instances and the obtained results are summarized in Tables V and VI.

Since the set $\mathcal{A}_i = [0, 2\pi]$ for all $i = 1, 2, \dots, n$ in problem (3), relaxation (ECSDR) is equivalent to (CSDR), as discussed

TABLE VII
CPU TIME OF ECSDR-BB AND SD [26] FOR SOLVING MIMO
DETECTION PROBLEM (1) WITH $M = 8$.

Problem Setup (m, n, M)		Average Performance		Worst-Case Performance	
	SNR	ECSDR-BB	SD	ECSDR-BB	SD
(30, 20, 8)	25	0.756	0.006	3.199	0.155
(30, 20, 8)	20	2.289	0.004	4.363	0.006
(30, 20, 8)	15	4.533	0.020	8.818	0.071
(30, 20, 8)	10	22.699	0.991	130.547	4.527
(30, 20, 8)	5	45.675	105.955	142.117	2004.779
(24, 20, 8)	25	2.954	0.004	6.471	0.005
(24, 20, 8)	20	4.685	0.012	8.385	0.091
(24, 20, 8)	15	8.313	0.325	27.128	1.781
(24, 20, 8)	10	52.040	25.201	183.207	627.656
(24, 20, 8)	5	70.287	566.220	196.828	10825.587
(20, 20, 8)	25	5.477	5.744	9.313	246.148
(20, 20, 8)	20	7.136	17.862	14.032	320.032
(20, 20, 8)	15	14.844	86.448	43.206	1922.981
(20, 20, 8)	10	102.886	281.456	433.586	5543.505
(20, 20, 8)	5	139.449	1836.163	571.820	14263.330

at the end of Section II and as demonstrated and verified in Table V. However, (ECSDR) still plays an important role of globally solving problem (3) in the ECSDR-BB algorithm, where the quality of (ECSDR) defined over the recursively partitioned subsets of \mathcal{A}_i becomes better and better.

As shown in Table VI, our proposed ECSDR-BB algorithm is quite efficient for solving small-scale problem instances (e.g., with $n \leq 10$). Moreover, the ECSDR-BB algorithm is able to solve all of problem instances within 602 iterations and within 268 seconds (on average). These results show the high efficiency of our proposed algorithm in solving the virtual beamforming design problem (3). By using our proposed algorithm as the benchmark, we can see that the two relaxations (for the original problem (3)) are generally not tight for the virtual beamforming design problem but the relaxation gaps are generally very small. We shall further compare the efficiency of our proposed ECSDR-BB algorithm with the general-purpose global optimization solver for solving the virtual beamforming design problem (3) in Section IV-E.

D. Comparison of ECSDR-BB with SD for MIMO Detection

In this subsection, we compare our proposed ECSDR-BB algorithm with the state-of-the-art tailored global algorithm called sphere decoder⁶ (SD) [27] for solving the MIMO detection problem (1). To compare the two algorithms, we generate problem instances with $M = 8$ and $M = 4$, and different (m, n) and different SNRs. In each setup, we generate 50 problem instances and apply the two algorithms to solve them. Numerical results of the average and worst-case CPU time of the 50 instances are summarized in Table VII and Table VIII.

For the case where $M = 8$, we can observe, from Table VII, that our proposed ECSDR-BB algorithm is not as efficient

⁶The code of the SD algorithm is downloadable from <https://www.mathworks.cn/matlabcentral/fileexchange/22890-sphere-decoder-for-mimo-systems>. We have made some modifications on the above downloaded code to improve its efficiency by adopting the techniques proposed in [26].

TABLE VIII
CPU TIME OF ECSDR-BB AND SD [26] FOR SOLVING MIMO
DETECTION PROBLEM (1) WITH $M = 4$.

Problem Setup (m, n, M)		Average Performance		Worst-Case Performance	
(m, n, M)	SNR	ECSDR-BB	SD	ECSDR-BB	SD
(24, 20, 4)	15	0.634	0.003	0.957	0.027
(36, 30, 4)	15	2.046	0.008	2.819	0.041
(48, 40, 4)	15	4.912	0.421	6.122	8.151
(60, 50, 4)	15	11.799	0.304	14.204	5.223
(24, 20, 4)	10	1.085	0.045	3.164	0.129
(36, 30, 4)	10	4.216	0.922	12.135	5.643
(48, 40, 4)	10	14.780	8.827	26.824	46.277
(60, 50, 4)	10	40.575	106.892	145.908	328.158
(20, 20, 4)	15	0.835	0.386	1.149	1.934
(22, 22, 4)	15	1.193	0.398	1.573	2.204
(24, 24, 4)	15	1.331	3.948	1.788	20.830
(26, 26, 4)	15	1.753	7.853	3.200	38.066
(28, 28, 4)	15	1.958	18.704	2.959	210.623
(20, 20, 4)	10	1.857	0.653	4.509	2.962
(22, 22, 4)	10	3.322	3.270	8.068	12.719
(24, 24, 4)	10	2.634	9.061	5.244	34.818
(26, 26, 4)	10	6.523	20.186	17.873	188.251
(28, 28, 4)	10	7.872	34.918	19.456	224.493

as SD for problems where $n = 20$, $m \geq 24$, and $\text{SNR} \geq 10$. However, the ECSDR-BB algorithm performs faster than the SD algorithm over the whole range of tested SNRs in the case where $(m, n) = (20, 20)$. Moreover, the ECSDR-BB algorithm becomes much faster than the SD algorithm in the low SNR case where $\text{SNR} = 5$. The reasons behind the above simulation results might be as follows. In the case where m is much larger than n , the matrix $\mathbf{H}^\dagger \mathbf{H}/m$ tends to be close to the $n \times n$ identity matrix \mathbf{I}_n . In this case, since $\mathbf{H}^\dagger \mathbf{H} \approx m\mathbf{I}_n$, we have

$$\frac{1}{2} \|\mathbf{H}\mathbf{x} - \mathbf{r}\|_2^2 \approx \frac{m}{2} \mathbf{x}^\dagger \mathbf{x} - \text{Re}(\mathbf{x}^\dagger \mathbf{H}^\dagger \mathbf{r}) + \frac{1}{2} \mathbf{r}^\dagger \mathbf{r}, \quad (29)$$

and thus the global solution of the original problem is very close to $\text{Scale}(\mathbf{H}^\dagger \mathbf{r}, \mathbf{e}_n)$, where $\text{Scale}(\cdot, \cdot)$ is defined in (15) and \mathbf{e}_n is the all-one vector of dimension n . Based on the above observation, a SD variant in [26], which applies a depth first search and selects the node according to an increasing distance from $\mathbf{H}^\dagger \mathbf{r}$ at each iteration, achieves a very high efficiency. However, for the cases with a fixed n , as m decreases, $\text{Scale}(\mathbf{H}^\dagger \mathbf{r}, \mathbf{e}_n)$ might not be a good estimator of the global solution of the original problem and hence the performance of the SD variant degrades very quickly, especially in the low SNR cases.

We can make the same observation on the comparison of the ECSDR-BB and SD algorithms from the results in Table VIII where $M = 4$. In particular, the SD algorithm performs better than the ECSDR-BB algorithm in the easy cases, whereas the performance of the SD algorithm sharply degrades when the problems become hard and the ECSDR-BB algorithm performs much better than the SD algorithm in the hard cases.

In short summary, our proposed ECSDR-BB algorithm performs very well in the hard cases, i.e., the number of inputs and outputs is equal or the SNR is low. Numerical results in Table VII and Table VIII show that our proposed ECSDR-BB algorithm exhibits a very promising performance in solving the MIMO channel detection problem (1) in the hard cases. It

is worth mentioning that the SD algorithm/variant is specially designed to solve the MIMO detection problem and it seems (at least to us) not trivial to extend it to solve more general problems while our proposed ECSDR-BB algorithm is able to solve various problems in the form of (CQP), with continuous and/or discrete argument constraints.

E. Comparison of ECSDR-BB with Baron for Virtual Beamforming Design

In this subsection, to further demonstrate the efficiency of our proposed ECSDR-BB algorithm, we compare it with Baron (version 18.8.24) [25], a well-known general-purpose global optimization solver, by applying them to solve the virtual beamforming design problem⁷ (3). Notice that Baron is also a branch-and-bound algorithm but it is based on linear programming relaxation. To apply Baron to solve problem (3), we need to first transform the problem into a real quadratic problem by representing the real and imaginary parts of each complex variable with two independent real variables. The error tolerances in both the ECSDR-BB algorithm and Baron are set to 10^{-4} . In our simulations, we generate 10 problem instances with $n = 5$ and 10 problem instances with $n = 10$ as done in Section V-C.

Table IX shows the numerical results for the 10 problem instances with $n = 5$. We can observe from the table that (ECSDR) is tight in this case and the ECSDR-BB algorithm terminates in only one iteration within 0.11 seconds; but Baron needs significantly larger number of iterations (i.e., in the order of 1000–10000) and more CPU time (i.e., from 41 to 432 seconds). Moreover, we have further compared the two algorithms on 10 problem instances with $n = 10$. However, we found that Baron fails to solve most of problem instances with $(m, n) = (10, 10)$ within 60 minutes (and thus the results are not listed here). In contrast, the ECSDR-BB algorithm can successfully solve problem instances with $m \in \{5, 10, 15\}$ and $n = 10$ within 6 seconds (on average), as listed in Table VI. These results clearly show that the specially designed ECSDR-BB algorithm achieves significantly higher efficiency on globally solving problem (CQP) than the general-purpose global optimization solver such as Baron.

VI. CONCLUSIONS

In this paper, we considered a class of nonconvex complex quadratic programming problems (i.e., problem (CQP)), which finds many important signal processing applications. We first derived a new enhanced relaxation (ECSDR) (compared to the conventional relaxation (CSDR)) for problem (CQP) based on the polar coordinate representations of the complex variables. Then we proposed a branch-and-bound global algorithm, ECSDR-BB, for solving problem (CQP) based on the newly derived relaxation. To the best of our knowledge, our proposed ECSDR-BB algorithm is the first tailored algorithm for problem (CQP) which is guaranteed to find the global solution of the problem (within any given error tolerance). We

⁷There is no existing specially designed global algorithm for the virtual beamforming design problem (3) that we can compare our algorithm with.

TABLE IX
NUMERICAL RESULTS OF ECSDR-BB AND BARON FOR VIRTUAL
BEAMFORMING DESIGN PROBLEM (3) WITH $n = 5$

Setup (m, n)	ECSDR-BB			Baron		
	ObjVal	# Iter	Time	ObjVal	# Iter	Time
(5, 5)	102.97	1	0.06	102.97	1567	80.0
(5, 5)	122.66	1	0.11	122.66	981	41.9
(5, 5)	91.40	1	0.11	91.40	1729	62.7
(5, 5)	120.71	1	0.11	120.71	967	60.8
(5, 5)	98.62	1	0.08	98.62	1705	66.4
(10, 5)	300.10	1	0.08	300.10	1855	80.3
(10, 5)	141.27	1	0.09	141.27	4071	208.7
(10, 5)	150.20	1	0.08	150.20	10009	431.7
(10, 5)	135.02	1	0.06	135.02	6999	322.8
(10, 5)	166.03	1	0.07	166.03	2477	86.2

applied our proposed ECSDR-BB algorithm for solving the MIMO detection problem, the unimodular radar code design problem, and the virtual beamforming design problem, and our simulation results show the high effectiveness of our proposed enhanced relaxation (ECSDR) and the high efficiency of our proposed ECSDR-BB algorithm. In particular, our proposed ECSDR-BB algorithm performs significantly better than the state-of-the-art SD algorithm for solving the MIMO detection problem in the hard cases (where the number of inputs and outputs is equal or the SNR is low) and the state-of-the-art general-purpose global solver Baron for solving the virtual beamforming design problem.

APPENDIX A PROOF OF PROPOSITION 3

Proof of (11): By the definition of $\mathcal{G}_{\mathcal{A}_i}$ (cf. (6)), we only need to show

$$|x_i| \geq r_i \cos\left(\frac{\bar{\theta}_i - \underline{\theta}_i}{2}\right). \quad (30)$$

Let us first consider the special case where $\mathcal{A}_i = [\underline{\theta}_i, \bar{\theta}_i]$. Without loss of generality, let us assume $r_i > 0$ in (30). (Otherwise, if $r_i = 0$, then $|x_i| \leq r_i = 0$ holds and thus (11) holds.) Since $(x_i, r_i) \in \mathcal{G}_{\mathcal{A}_i}$, we have

$$\alpha_i \text{Re}(x_i) + \beta_i \text{Im}(x_i) \geq \gamma_i r_i, \quad (31)$$

where α_i, β_i , and γ_i are given in (7), which further implies

$$\alpha_i \text{Re}(x_i) + \beta_i \text{Im}(x_i) \leq \sqrt{[\alpha_i^2 + \beta_i^2] [\text{Re}^2(x_i) + \text{Im}^2(x_i)]} = |x_i|. \quad (32)$$

Combining (31) and (32) with the definition of γ_i shows that (30) holds for all $(x_i, r_i) \in \mathcal{G}_{[\underline{\theta}_i, \bar{\theta}_i]}$.

Now let us consider the general case where \mathcal{A}_i is any set satisfying $\mathcal{A}_i \subseteq [\underline{\theta}_i, \bar{\theta}_i]$. Since the convex envelope of \mathcal{A}_i must also be a subset of that of $[\underline{\theta}_i, \bar{\theta}_i]$, we have $\mathcal{G}_{\mathcal{A}_i} \subseteq \mathcal{G}_{[\underline{\theta}_i, \bar{\theta}_i]}$. From this and the result for the case where $\mathcal{A}_i = [\underline{\theta}_i, \bar{\theta}_i]$, we can conclude that (30) holds for all $(x_i, r_i) \in \mathcal{G}_{\mathcal{A}_i}$.

Proof of (12): By the definition of $\mathcal{F}_{\mathcal{B}_i}$ (cf. (9)), we only need to show the second inequality in (12). Since $X_{ii} - (\ell_i + u_i)r_i + \ell_i u_i \leq 0$ holds for all $(X_{ii}, r_i) \in \mathcal{F}_{\mathcal{B}_i}$, it follows

$$\begin{aligned} X_{ii} - r_i^2 &\leq (\ell_i + u_i)r_i - \ell_i u_i - r_i^2 \\ &= \frac{(u_i - \ell_i)^2}{4} - \left(r_i - \frac{\ell_i + u_i}{2}\right)^2 \\ &\leq \frac{(u_i - \ell_i)^2}{4}. \end{aligned}$$

APPENDIX B PROOF OF THEOREM 2

At the beginning of the k -th iteration of the ECSDR-BB algorithm, the initial feasible set \mathcal{D}^0 has been (recursively) partitioned into k smaller subsets. Since the global solution of problem (CQP) must lie in one of the subsets and L^k is the smallest lower bound of all subproblems in the active node set \mathcal{P} , we have $L^k \leq \nu^*$. Since $\hat{\mathbf{x}}^k = \text{Scale}(\mathbf{x}^k, \mathbf{r}^k)$ (cf. (15)) is feasible to problem (CQP), we immediately get $\nu^* \leq F(\hat{\mathbf{x}}^k)$. Combining the above two inequalities yields (18).

Next, we prove that the returned solution \mathbf{x}^* by the ECSDR-BB algorithm is an ϵ -optimal solution. It follows from (16) and (18) that $F(\hat{\mathbf{x}}^k) \leq L^k + \epsilon \leq \nu^* + \epsilon$. By the update rule of the upper bound (cf. Line 19 of the ECSDR-BB algorithm), U^* must satisfy $U^* \leq F(\hat{\mathbf{x}}^k)$. Hence, for the returned solution \mathbf{x}^* , there holds $F(\mathbf{x}^*) = U^* \leq \nu^* + \epsilon$, which, together with Definition 1, shows that \mathbf{x}^* is an ϵ -optimal solution of problem (CQP).

APPENDIX C PROOF OF LEMMA 1

By the definition of $F(\mathbf{x})$ in problem (CQP), we have

$$\begin{aligned} &F(\hat{\mathbf{x}}^k) - L^k \\ &= F(\hat{\mathbf{x}}^k) - \frac{1}{2} \mathbf{Q} \bullet \mathbf{X}^k - \text{Re}(\mathbf{c}^\dagger \mathbf{x}^k) \\ &\leq |F(\hat{\mathbf{x}}^k) - F(\mathbf{x}^k)| + \left| F(\mathbf{x}^k) - \frac{1}{2} \mathbf{Q} \bullet \mathbf{X}^k - \text{Re}(\mathbf{c}^\dagger \mathbf{x}^k) \right| \\ &= |F(\hat{\mathbf{x}}^k) - F(\mathbf{x}^k)| + \left| \frac{1}{2} \mathbf{Q} \bullet (\mathbf{X}^k - \mathbf{x}^k (\mathbf{x}^k)^\dagger) \right|. \end{aligned}$$

Next, we bound the two terms $|F(\hat{\mathbf{x}}^k) - F(\mathbf{x}^k)|$ and $|\mathbf{Q} \bullet (\mathbf{X}^k - \mathbf{x}^k (\mathbf{x}^k)^\dagger)|$ from the above one by one.

We first bound the term $|F(\hat{\mathbf{x}}^k) - F(\mathbf{x}^k)|$. It follows directly from (21) that

$$|F(\mathbf{x}^k) - F(\hat{\mathbf{x}}^k)| \leq M_F \|\mathbf{x}^k - \hat{\mathbf{x}}^k\|_2. \quad (33)$$

By the definition of S_1^* (cf. (17)), we immediately get

$$\|\mathbf{x}^k - \hat{\mathbf{x}}^k\|_2 \leq \sqrt{n} S_1^*. \quad (34)$$

Combining (33) and (34) gives

$$|F(\mathbf{x}^k) - F(\hat{\mathbf{x}}^k)| \leq \sqrt{n} M_F S_1^*. \quad (35)$$

Now, we bound the term $|\mathbf{Q} \bullet (\mathbf{X}^k - \mathbf{x}^k (\mathbf{x}^k)^\dagger)|$. Clearly, there holds

$$\begin{aligned} &|\mathbf{Q} \bullet (\mathbf{X}^k - \mathbf{x}^k (\mathbf{x}^k)^\dagger)| \\ &\leq \|\mathbf{Q}\|_F \left\| (\mathbf{X}^k - \mathbf{x}^k (\mathbf{x}^k)^\dagger) \right\|_F. \end{aligned} \quad (36)$$

Let $\lambda_{\max} \geq 0$ be the largest eigenvalue of the positive semidefinite matrix $\mathbf{X}^k - \mathbf{x}^k (\mathbf{x}^k)^\dagger$. Then, we have

$$\begin{aligned} & \left\| \mathbf{X}^k - \mathbf{x}^k (\mathbf{x}^k)^\dagger \right\|_{\text{F}} \\ & \leq \sqrt{n} \lambda_{\max} \leq \sqrt{n} \text{Trace} \left(\mathbf{X}^k - \mathbf{x}^k (\mathbf{x}^k)^\dagger \right). \end{aligned} \quad (37)$$

By the definitions of S_1^* and S_2^* (cf. (17)), we have

$$\begin{aligned} & \text{Trace} \left(\mathbf{X}^k - \mathbf{x}^k (\mathbf{x}^k)^\dagger \right) \\ & = \sum_{i=1}^n \left(X_{ii}^k - |x_i^k|^2 \right) \\ & = \sum_{i=1}^n \left[\left(X_{ii}^k - (r_i^k)^2 \right) + (r_i^k + |x_i^k|) (r_i^k - |x_i^k|) \right] \\ & \leq n \left[\left(X_{i_2^* i_2^*}^k - (r_{i_2^*}^k)^2 \right) + 2u_{\max} \left(r_{i_1^*}^k - |x_{i_1^*}^k| \right) \right] \\ & = n (S_2^* + 2u_{\max} S_1^*), \end{aligned}$$

which, together with (36) and (37), further implies

$$\left| \mathbf{Q} \bullet \left(\mathbf{X}^k - \mathbf{x}^k (\mathbf{x}^k)^\dagger \right) \right| \leq \|\mathbf{Q}\|_{\text{F}} n^{\frac{3}{2}} (S_2^* + 2u_{\max} S_1^*). \quad (38)$$

From (35), (38), and the definitions of M_1 and M_2 (cf. (22) and (23)), we immediately get the desired inequality in (24).

APPENDIX D PROOF OF LEMMA 2

It follows from Theorem 2 that, to prove the lemma we only need to prove that (16) holds under (C1), (C2), or (C3).

If condition (C1) holds, then it follows from (24) that

$$F(\hat{\mathbf{x}}^k) - L^k \leq (M_1 + M_2) S_1^*. \quad (39)$$

In this case, we have $\hat{x}_{i_1^*}^k = r_{i_1^*}^k e^{i \arg(x_{i_1^*}^k)}$ (cf. (15)) and thus

$$\left| \hat{x}_{i_1^*}^k - x_{i_1^*}^k \right| = r_{i_1^*}^k - |x_{i_1^*}^k|. \quad (40)$$

Then, we have

$$\begin{aligned} S_1^* & = \left| \hat{x}_{i_1^*}^k - x_{i_1^*}^k \right| = r_{i_1^*}^k - |x_{i_1^*}^k| \\ & \leq r_{i_1^*}^k \left[1 - \cos \left(\frac{\bar{\theta}_{i_1^*}^k - \underline{\theta}_{i_1^*}^k}{2} \right) \right] \\ & \leq \frac{u_{\max} \left(\bar{\theta}_{i_1^*}^k - \underline{\theta}_{i_1^*}^k \right)^2}{8} \leq \frac{u_{\max} \kappa_1^2}{8}, \end{aligned} \quad (41)$$

where the first equality is due to the definition of S_1^* (cf. (17)), the second equality comes from (40), the first inequality is due to (11), and the second inequality is a result of the definition of u_{\max} (cf. (19)) and the inequality $1 - \cos(\theta) \leq \frac{\theta^2}{2}$ for all $\theta \in \mathbb{R}$, and the last inequality follows from condition (C1). Combining (39), (41), and the definition of κ_1 (cf. (25)) yields the desired result in (16).

If condition (C2) holds, then we can show $S_1^* = S_2^* = 0$. By this and (24), we obtain $F(\hat{\mathbf{x}}^k) - L^k \leq 0$, which further implies (16).

If condition (C3) holds, then it follows from (24) that

$$F(\hat{\mathbf{x}}^k) - L^k \leq (M_1 + M_2) S_2^*. \quad (42)$$

Moreover, from (12) and the definition of S_2^* (cf. (17)), we obtain $S_2^* = X_{i_2^* i_2^*}^k - r_{i_2^*}^2 \leq \left(u_{i_2^*}^k - \ell_{i_2^*}^k \right)^2 / 4$. This, together with (42), (C3), and the definition of κ_2 (cf. (26)), shows the desired result in (16).

APPENDIX E PROOF OF THEOREM 3

We consider two sets \mathcal{A}_i and \mathcal{B}_i separately. Moreover, when we consider set \mathcal{A}_i , we consider two cases where \mathcal{A}_i is an interval and a discrete set separately.

We first consider the case where \mathcal{A}_i is an interval. We show that the set \mathcal{A}_i will be partitioned into at most $\mu(\mathcal{A}_i)$ of subsets before the algorithm terminates, where $\mu(\mathcal{A}_i)$ is defined in (28). According to the algorithm, suppose that $S_1^* \geq S_2^*$ at the k -th iteration, then the interval $\mathcal{A}_{i_1^*}^k$ will be partitioned into two subsets with the same length. If the ECSDR-BB algorithm does not terminate in Line 12 at the k -th iteration, then it follows from condition (C1) in Lemma 2 that $\omega(\mathcal{A}_{i_1^*}^k) > \min\{\kappa_1, \pi\}$ and the length of each subset obtained after the partition is larger than $\frac{1}{2} \min\{\kappa_1, \pi\}$. Hence, if set \mathcal{A}_i has been partitioned into $\mu(\mathcal{A}_i)$ of subsets, the total length of all obtained subsets is strictly greater than

$$\mu(\mathcal{A}_i) \frac{1}{2} \min\{\kappa_1, \pi\} \geq \omega(\mathcal{A}_i),$$

where the inequality is due to the definition of $\mu(\mathcal{A}_i)$ (cf. (28)). This is a contradiction. Therefore, if \mathcal{A}_i is an interval, it can be partitioned at most $\mu(\mathcal{A}_i)$ times before the algorithm terminates.

Now, we consider the case where \mathcal{A}_i is a discrete set (with a finite number of elements). We can use the similar argument as in the above case to show that \mathcal{A}_i can be partitioned at most $\mu(\mathcal{A}_i) = |\mathcal{A}_i|$ times. The only difference here is that \mathcal{A}_i is a discrete set. More specifically, according to the algorithm, suppose that $S_1^* \geq S_2^*$ at the k -th iteration, then the interval $\mathcal{A}_{i_1^*}^k$ will be partitioned into two nonempty and nonoverlapping subsets. If the ECSDR-BB algorithm does not terminate in Line 12 at the k -th iteration, then it follows from condition (C2) in Lemma 2 that $\mathcal{A}_{i_1^*}^k$ is not a singleton and each subset obtained after the partition is not empty. Hence, if \mathcal{A}_i is a discrete set, it can be partitioned at most $|\mathcal{A}_i|$ times before the algorithm terminates.

Finally, we consider set \mathcal{B}_i . This case is essentially the same as the case where \mathcal{A}_i is an interval. Using the same argument, we can show that the set \mathcal{B}_i can be partitioned at most $\max \left\{ \left\lceil \frac{2\omega(\mathcal{B}_i)}{\kappa_2} \right\rceil, 1 \right\}$ times before the algorithm terminates.

From the above analysis, we can conclude that the proposed algorithm must terminate within at most K_ϵ iterations, where K_ϵ is defined in (27).

REFERENCES

- [1] C. Lu, Y.-F. Liu, and J. Zhou, "An efficient global algorithm for non-convex complex quadratic problems with applications in wireless communications," in *Proc. IEEE/CIC Int. Conf. Commun. China (ICCC)*, Oct. 2017, pp. 1–5.
- [2] J. Jaldén, C. Martin, and B. Ottersten, "Semidefinite programming for detection in linear systems—Optimality conditions and space-time decoding," in *Proc. IEEE Int. Conf. Acoust. Speech Signal Process. (ICASSP)*, Apr. 2003, pp. 9–12.

- [3] W.-K. Ma, P.-C. Ching, and Z. Ding, "Semidefinite relaxation based multiuser detection for M -ary PSK multiuser systems," *IEEE Trans. Signal Process.*, vol. 52, no. 10, pp. 2862–2872, Oct. 2004.
- [4] A. D. Maio, S. D. Nicola, Y. Huang, Z.-Q. Luo, and S. Zhang, "Design of phase codes for radar performance optimization with a similarity constraint," *IEEE Trans. Signal Process.*, vol. 57, no. 2, pp. 610–621, Feb. 2009.
- [5] A. D. Maio, Y. Huang, M. Piezzo, S. Zhang, and A. Farina, "Design of optimized radar codes with a peak to average power ratio constraint," *IEEE Trans. Signal Process.*, vol. 59, no. 6, pp. 2683–2697, Jun. 2011.
- [6] M. Soltanalian and P. Stoica, "Designing unimodular codes via quadratic optimization," *IEEE Trans. Signal Process.*, vol. 62, no. 5, pp. 1221–1234, Mar. 2014.
- [7] M. Hong, Z. Xu, M. Razaviyayn, and Z.-Q. Luo, "Joint user grouping and linear virtual beamforming: Complexity, algorithms and approximation bounds," *IEEE J. Sel. Areas Commun.*, vol. 31, no. 10, pp. 2013–2027, Oct. 2013.
- [8] I. Waldspurger, A. d'Aspremont, and S. Mallat, "Phase recovery, Max-Cut and complex semidefinite programming," *Math. Program.*, vol. 149, no. 1–2, pp. 47–81, Feb. 2015.
- [9] W. Pu, Y.-F. Liu, J. Yan, H. Liu, and Z.-Q. Luo, "Optimal estimation of sensor biases for asynchronous multi-sensor data fusion," *Math. Program.*, vol. 170, no. 1, pp. 357–386, 2018.
- [10] A. S. Bandeira, N. Boumal, and A. Singer, "Tightness of the maximum likelihood semidefinite relaxation for angular synchronization," *Math. Program.*, vol. 163, no. 1–2, pp. 145–167, May 2017.
- [11] Z.-Q. Luo, W.-K. Ma, A. M.-C. So, Y. Ye, and S. Zhang, "Semidefinite relaxation of quadratic optimization problems," *IEEE Signal Process. Mag.*, vol. 27, no. 3, pp. 20–34, May 2010.
- [12] D. P. Palomar and Y. C. Eldar, *Convex Optimization in Signal Processing and Communications*. New York, USA: Cambridge University Press, 2010.
- [13] A. M.-C. So, J. Zhang, and Y. Ye, "On approximating complex quadratic optimization problems via semidefinite programming relaxations," *Math. Program.*, vol. 110, no. 1, pp. 93–110, Jun. 2007.
- [14] S. Zhang and Y. Huang, "Complex quadratic optimization and semidefinite programming," *SIAM J. Optim.*, vol. 16, no. 3, pp. 871–890, 2006.
- [15] C. Lu, Z. Deng, W.-Q. Zhang, and S.-C. Fang, "Argument division based branch-and-bound algorithm for unit-modulus constrained complex quadratic programming," *J. Global Optim.*, vol. 70, no. 1, pp. 171–187, Jan. 2018.
- [16] M. X. Goemans and D. P. Williamson, "Improved approximation algorithms for maximum cut and satisfiability problems using semidefinite programming," *J. ACM*, vol. 42, no. 6, pp. 1115–1145, Nov. 1995.
- [17] —, "Approximation algorithms for Max-3-Cut and other problems via complex semidefinite programming," *J. Comput. Syst. Sci.*, vol. 68, no. 2, pp. 442–470, Mar. 2004.
- [18] F. Jarre, F. Lieder, Y.-F. Liu, and C. Lu, "Set-completely-positive representations and cuts for the max-cut polytope and the unit modulus lifting," *J. Global Optim.*, vol. 76, no. 4, pp. 913–932, 2020.
- [19] A. B. Gershman, N. D. Sidiropoulos, S. Shahbazpanahi, M. Bengtsson, and B. Ottersten, "Convex optimization-based beamforming," *IEEE Signal Process. Mag.*, vol. 27, no. 3, pp. 62–75, May 2010.
- [20] S. He, Z.-Q. Luo, J. Nie, and S. Zhang, "Semidefinite relaxation bounds for indefinite homogeneous quadratic optimization," *SIAM J. Optim.*, vol. 19, no. 2, pp. 503–523, 2008.
- [21] Z.-Q. Luo, N. D. Sidiropoulos, P. Tseng, and S. Zhang, "Approximation bounds for quadratic optimization with homogeneous quadratic constraints," *SIAM J. Optim.*, vol. 18, no. 1, pp. 1–28, 2007.
- [22] R. Ge, F. Huang, C. Jin, and Y. Yuan, "Escaping from saddle points – online stochastic gradient for tensor decomposition," in *Proc. The 28th Conference on Learning Theory (COLT)*, Jul. 2015, pp. 797–842.
- [23] C. Lu, Y.-F. Liu, W.-Q. Zhang, and S. Zhang, "Tightness of a new and enhanced semidefinite relaxation for MIMO detection," *SIAM J. Optim.*, vol. 29, no. 1, pp. 719–742, 2019.
- [24] J. Linderoth, "A simplicial branch-and-bound algorithm for solving quadratically constrained quadratic programs," *Math. Program.*, vol. 103, no. 2, pp. 251–282, Jun. 2005.
- [25] M. Tawarmalani and N. V. Sahinidis, "A polyhedral branch-and-cut approach to global optimization," *Math. Program.*, vol. 103, no. 2, pp. 225–249, Jun. 2005.
- [26] A. M. Chan and I. Lee, "A new reduced-complexity sphere decoder for multiple antenna systems," in *Proc. IEEE Int. Conf. Commun. (ICC)*, Apr.-May 2002, pp. 460–464.
- [27] O. Damen, A. Chkeif, and J.-C. Belfiore, "Lattice code decoder for space-time codes," *IEEE Commun. Lett.*, vol. 4, no. 5, pp. 161–163, May 2000.
- [28] A. Ben-Tal and A. Nemirovski, *Lectures on Modern Convex Optimization*. Philadelphia, PA, USA: SIAM, 2001.
- [29] C. Lu and Y.-F. Liu, "An efficient global algorithm for single-group multicast beamforming," *IEEE Trans. Signal Process.*, vol. 65, no. 14, pp. 3761–3774, Jul. 2017.
- [30] J. F. Sturm, "Using SeDuMi 1.02, A MATLAB toolbox for optimization over symmetric cones," *Optim. Methods Softw.*, vol. 11, no. 1–4, pp. 625–653, 1999.